POLITECNICO DI TORINO

MASTER THESIS

A Heuristic Optimization Method For Retrofitting Structures Using FRP

Candidate:

Luis Alberto

BOHÓRQUEZ GRATERON

Supervisor:

Gian Paolo

CIMELLARO

2021

"Dreams Don't Work Unless You Do."

John C. Maxwell

Abstract

Seismic motions have been challenging structural engineers for decades by testing the performance of building structures. For this reason, mainly, existing and heritage buildings are prone to develop issues concerning stability during a ground motion. Retrofitted techniques (e.g. CAM, shear walls, steel, and concrete jacketing) have been thriving to diminish structural design's flawed conception. However, the disadvantages of invasive techniques or either geometrical or site problems dare to select an appropriate approach. Fiber-reinforced polymers rise among the strategies by overcoming common issues. Significant accomplishments have been attained by research designing the strategy to fulfill the use of FRP in RC structures adequately; nonetheless, a few addresses the optimal methodology to implement FRP layout in columns. This thesis presents a heuristic approach to locate the FRP material in columns and joints to reduce the inter-story drift and considering the uniformity of these along with the height. The approach is defined by a series of iteration in a generic algorithm where the structures is assessed with non-linear Time- History (NTHA). The proposed methodology has been tested in three non-ductile RC buildings subjected to far-fault and near-fault ground motion where the structures exhibit an improvement regarding the seismic performance.

Keywords: FRP, retrofitting techniques, RC structures, optimization

Acknowledgments

This dissertation ends a phase of my career after successfully achieving each goal of each challenge that I encountered in the path. Therefore, the gratitude exerted after obtaining the so awaited goal entails me to appreciate the people that surrounded me in all the way.

To both of my academic institutions, to the Universidad Central de Venezuela, which received me and guided me through each of the required knowledge of my career, whose professors gave everything and dedicated hours of teaching to prepare me to overcome the shadows—to the Politecnico di Torino, allowing me to embrace the opportunity to live a phenomenal international experience, which professors shepherded through new subjects and boosted me until the end of this period.

Special thanks to my Academic Supervisor, prof. Gian Paolo Cimerallo, whose support and advice led me straight to my objective. Whose availability, even in the days of great concern, brought a passion for the research. Besides, I am entirely grateful to my Academic Advisor, prof. Christopher Mendoza, whose advice was addressed to my development, not just professionally but humanly.

To all the friends that these institutions left me, as there is no achievement without friends. Especially for those who saw me thrived at the very beginning, Diego Coronado, David Acevedo, Daniel Benaim, Reinaldo Mansilla, Andrea

Rivero, and Nazareth Carrero. For those, the magnificent city of Turin left me, Rosangela Itriago, Estefania Mujica, Juliana Ortiz, Felipe Carvajal, and Luis Miguel Hernández.

To my brothers, Luis Alejandro and Luis Alfonso, and especially to my parents, Luis Alfonso Bohórquez and Milagros del Valle Grateron, whose support cannot be quantified, whose hands were always there for me. All that you gave me along these years brought joy to my life and pushed me to become the best of me. Therefore, there will never be something to retrieve how grateful I am.

Torino, February 14, 2021 L. B.

Table of Content

List of Figures

List of Tables

Nomenclature

Acronyms

FEA	finite element analysis
FEM	finite element method
FRP	fiber-reinforced polymer
EA	evolutionary algorithm
GA	genetic algorithm
NSGA	non-dominated sorting genetic algorithm
OC	optimality criteria
ULS	ultimate limit state

Notations

E_c	unconfined concrete elasticity modulus
f_o	unconfined compressive strength of concrete
f_c	confined compressive strength of concrete
E_s	*steel* modulus of elasticity
f_y	yielding strength of steel
E_{fib}	fiber modulus of elasticity
E_{FRP}	fiber-reinforced polymer modulus of elasticity
f_f	tensile strength of the fiber-reinforced polymer
t	thickness of fiber-reinforced polymer sheet

h_{col}	height of column cross-section
b_{col}	width of column cross-section
h_{beam}	height of beam cross-section
b_{beam}	width of beam cross-section
h_{girder}	height of girder cross-section
b_{girder}	width of girder cross-section
H_n	height of story n
H_1	height of fisrt story
L_{bay}	length of bay
L_{frame}	length of frame
ρ_l	longitudinal reinforcement volumetric ratio
d_{bl}	diameter of longitudinal reinforcement
g	gap between sheet and end of column
ρ_K	stiffness ratio between FRP and concrete
ρ_ε	strain ratio between FRP and concrete

Dedicated to my parents…

Introduction

In human history, casualties have converged by several roots over time's path; these can be effortlessly classified as human-made and natural disasters. Even that human activities have a few highlighted events as World War I and World War II that brought a considerable death toll worldwide, the natural phenomenon does not stay behind. In particular, seismic events are considered as one of the most catastrophic records in human experience. The deadliest documented earthquakes threw our time-lapse to the 14th century. In 1556 AD, in Shaanxi, China, a full-motion hit, causing a loss of life that goes over 830.000 people.

Nonetheless, in recent years strong quakes have been causing detrimental effects as the Sumatra-Andaman earthquake brought massive tsunami waves destroying structures and life; over 230.000 human lives were lost. Lastly, Haiti's earthquake, which death toll was estimated to over 230.000. Without mentioning any other disastrous quake that will always be part of our memories, engineers have learned how to respect the natural phenomenon and prevent its harmful consequences in our lives.

Civil engineers have the rigorous task of dealing with this phenomenon; understanding the seismic motion and the interaction between soil-structure have been analyzed over several decades. Even though the development in these areas has been vast, researchers are still digging deep to overcome earthquakes' dangerous occurrence. The problem arises when the need for conservation begins to have an essential role in human life. Historical buildings and architectural heritage have been defined by their cultural richness, where the preservation of the structure is required. Most of these structures are expected to have a low seismic resistance because of poor design. This is addressed to the lack of knowledge of the ground motion effect. Hence, the assessment of these structures gathers the necessary information to verify whether the structure is currently stable or needs intervention to enhance its performance.

Several techniques can be implemented to improve the seismic performance of existance buildings, such as shear walls, concrete and steel jacketing, which increase the structure's stiffness but modify the entire behavior and are known to be destructive techniques. Instead of using classical techniques, fiber-reinforced polymers have been implemented as a retrofitting material. It has been claimed to excel in its implementation in-situ and increase the local and global structures' performance. However, the most substantial drawback is the cost of its use.

Therefore, the thesis proposes to develop a metaheuristic method that permits the use of an optimal FRP retrofitting layout by increase the lateral capacity and setting a uniform drift distribution along with the entire structure.

Motivation

Humankind has been known to find complex solutions thanks to the robust implementation of technology nowadays. Implementing an iteratively design or assessment of buildings in civil engineering reduces the time spent, which directly translates to a money-saving. The research's motivation is to merge the computation capacity in civil engineering retrofitting design and the lack of further investigation in the arrangement of different confinement schemes in columns and the strengthening of joints to lower the use of FRP material.

Objective

Main Objective

To develop a metaheuristic method to assess the optimal retrofitting strategy involving the use of FRP on columns and joints aiming to a reduction of the interstory drift.

Secondary objective

- To reduce the inter-story drift of RC building structure by mean of FRP retrofitting technique.
- To determine the uniform distribution of the inter-story drift by implementing FRP wrapping sheets in columns and joints.

- To decrease the experience dependence in FRP retrofitting technique implementation by assessing several FRP retrofitted columns arrangement in the structure.

Research questions

Evolutionary Algorithm has been increasing its use in civil engineering applications since notably enhancing time-saving in designing or assessing structures. Hence, new challenges drive engineers to develop different means to overcome not trivial criteria of structural performance. A metaheuristic approach can be implemented in FRP retrofitting scheme to search for an optimum layout by setting a uniform inter-story drift.

Thesis Organization

The current work is organized following a schematical deepens in knowledge: Chapter 1 details the researches efforts regarding the retrofitting optimization scheme of RC structures by implementing fiber-reinforced polymers sheets in the confinement of structural columns and the empirical findings realized towards the implementation of joints retrofitting approaches. Chapter 2 highlights the theoretical definition required to deepen the investigation, stressing the application of fiber-reinforced polymers in civil engineering, types, and mechanical performances to define genetic algorithm and its components. Chapter 3 describes the methodology implementation of the metaheuristic strategy for the retrofitting through FRP sheets in columns and joints. Chapter 4 describes the specific cases under investigation, a brittle space frame RC structure which must be retroffited to guaranteed seismic stability, and a set of archetype models which are subjected to near-fault and far-fault ground motions to which the retrofitting strategy is implemented in both cases and, additionally, the layout configuration in both, columns and joints, is depicted.

Chapter 1

Literature Review

In recent years, the performance of existing buildings has been a research field that engineers must take care of due to the possibility of leading to a tragic event. It has been found, thanks to the advances of technology, innovative techniques, and improvement of the structural design, that most of the existing buildings are not able to undergo a seismic event because of either inefficient resistance or ductility. Retrofitting schemes have been developed to overcome, in a safe manner, this ineffective or inadequate design. Fiber-reinforced polymer (FRP) has been employed successfully for years as it exceeds among other retrofitting strategies concerning the technique's applicability, nondestructive, and speediness.

Nowadays, FRP has been a recent investigation and development field due to its significant potential concerning the improvement of structural behavior under rare events. This technique's outstanding functionality leads to a worldwide application; however, the retrofitting scheme has been governed by experience most of the time. Concerning the optimal application of the FRP in a seismic event, Zou et al. (2007) investigated the performance-based FRP retrofitting in concrete frames, where the research aimed to create a suitable approach that optimizes the use of FRP material by being compared with the inelastic design drift of the structure. The procedure constitutes the utilization of Principal Virtual Work and Taylor Series for tracking the development of the plastic hinges in the frame and was successfully achieved by the integration of Optimality Criteria (OC). Recently, optimization techniques have been used in the structural assessment to achieve an optimum design. Choi et al. (2014) assessed a reinforced concrete frame with a method that optimizes the retrofitting scheme with shear-critical criteria. They proposed a strategy in which a Non-dominated Sorting Genetic Algorithm (NSGA-II) is employed to reduce the FRP material used to retrofit the columns considering an optimal placement by introducing the possibility to achieve the required flexural and shear strength. Furthermore, based on (NSGA-II), Choi (2017) explored the assessment methodology deemed the effective placement of (FRP) plies in beams and columns of a reinforced concrete frame, which led to a reduction of the FRP cost and reaching the prevention of the possible collapse of the structure. Similar work was realized by Chisari and Bedon (2016) where the optimization of the FRP sheets was compared at Damage and Near Collapse Limit State; subsequently, Chisari and Bedon (2017) developed a design approach by implementing the optimization process and the several Limit State drift criteria. Even though the investigation as mentioned above have been conducted reaching the optimum behavior with the use of FRP in comparison with the reduction of the drift of the system, a new strategy conducted by Mahdavi et al. (2019) steered the optimization process regarding the most advantageous FRP consumption and uniform distribution of the plastic hinges development, employing Genetic Algorithm (GA) and Particle Swarm Optimization (PSO). They concluded that the most favorable cost-efficient scenario is retrofitting the first story columns uniformly; however, it is not the best concerning the more significant material reduction. In the same way, innovative formulation leads to the research of Farinazzo (2019), by stating that a new advantageous criterion is to seek the optimal layout of the wrapped columns in the buildings by fixing the parameters of the FRP material. Nonetheless, a more recent field in FRP investigation is the retrofitting of external joints due to non-conforming features of detailing for seismic resistance. Several investigation have proven the benefits of nodes enhancement and set up of the retrofitting approach (Cosgun et al. 2019; Ilki et al. 2013; Pohoryles et al. 2019; Tsonos and Stylianidis 2002).

Among the exhaustive investigation made in this field, a lack of effort has been developed in the potential use of different FRP wrapping retrofitting schemes, with the possibility to couple this latter to the retrofitting of nodes and further enhance the seismic performance. Therefore, the development of a metaheuristic technique to assess the best solution in the layout of FRP confinement schemes is herein explained. The use of a more accurate distribution of the FRP material in the elements has been found to decrease the quantity of its implementation permitting achieving the optimal solution and the set goal, which is a uniform distribution along the inter-story drift.

Chapter 2

Theoretical Framework

2.1 Background works

The construction field is one of the industries that has remained in constant change as new methodologies, techniques, and materials successfully become reliable for their use in professional practice. However, these changes are spread well since the beginning of human history; engineers are headed in a chronological sphere by civil engineers, which are responsible for the safety of civilians. As the technologies of material had a boost upwards since the Industrial Revolution, in this particular aspect, the construction field took advantage of the advent of new prospects to be used in the design of structures. One of the most recent materials, known as *Fiber Reinforced Polymer* (FRP), is a material which characteristics excel among others as its high strength - weight ratio and high elasticity and resistance to alkaline environments. FRP efficiently manages to become a tendency in its use in construction; nonetheless, the cost is the most controversial aspect in the field. Besides this, several countries have been searching for new codes that regulate this material's proper use.

The structure's stability is a major challenge among structural engineers as a shortcoming in the design is exposed after a given phenomenon that causes the damage or even the collapse of the structure. The path of time and the acquired knowledge leads to the development or up-gradation codes to fulfill the structural demand. Nonetheless, existing buildings are usually found with no compliance with the new regulations, which is attributed directly to the lack of awareness of the subject. The effects of the seismic motion in a structure is a field of research in the engineering field that regrettably is not entirely covered in detail, and the new developments in the area are commonly accomplished by gathering information after being revealed in a seismic event, for instance, Caracas, Venezuela (1967), Mexico City, Mexico (1985), Kobe, Japan (1995), Chi-Chi, Taiwan (1999).

The effort of engineers to successfully design new resilient structures has been well recognized throughout history. However, this attempt has diverged directly to the existing buildings, as the codes have been modified through time, these structures commonly have no compliance with the new seismic requirements. The history of cities defines the line where structure becomes part of our memories, and hence, the architectural heritage is transformed into a significant challenge that engineers must tackle no matter the geometrical, physical, or even cultural limitations. Modifications of structural elements depend on the characteristics that have to be improved, either from a local or global perspective.

Retrofitting of a structure defines the structural system's modification before a given phenomenon regarding its strength, stiffness, stability, and ductility; in the case of earthquake motion, the specific term is commonly known as seismic retrofitting (Chakrabarti et al. 2008).

The correct assessment of an existing building will indicate the lack of strength, stiffness, or other feature for a given element or the entire system. Therefore, depending on the possible failure mechanism, a retrofitting technique or a combination of these will be conducted. A few can be mentioned among the possible retrofitting techniques, such as shear walls, concrete and steel jacketing, CAM, and finally, fiber-reinforced polymer (FRP). Every single one of them excels in specifics mechanical properties improving the performance of the structural system. Nonetheless, FRP has been gaining renown due to its great capacities, speediness of implementation, and reduction of the intrusive mechanism.

2.2 The fiber-reinforced polymer in civil engineering

Polymers have been enhanced for decades and have fulfilled requirements in different professional areas for their application and performance. FRP has been recognized as the optimum building material regarding corrosion resistance, lightweight, and versatility in manufacturing and site placement.

2.2.1 Commercial FRP EB retrofitting classification

As before-mentioned, *Fiber-reinforced polymers* is a versatile material that can be shaped in unique appropriate shapes for use in the structural field. Commercially speaking, in the case of retrofitting, externally bonded FRP can be classified depending on its delivery and installation in-situ. Several regulations define these types (ACI 2007; CNR 2013; fib 2006; fib 2007):

- *Wet layup systems* consist of FRP sheets or fabrics that are saturated with resin and cured. The application is composed of a saturated resin with primer and putty, which bonds the sheets to the surface. Nowadays, this procedure is divided *into dry unidirectional* or *bidirectional fiber sheets* and *fiber tows*.
- *Prepeg systems* are pre-impregnated FRP sheets that are partially cured. The FRP fibers or fabric are bonds to the surface with or without additional resin. In contrast with *wet layup systems*, these are saturated off-site and cured in place. It can also be divided into the same classification as before, which is *pre-impregnated unidirectional or bidirectional fiber sheets* and *fiber tows*.
- *Pre-cured systems* are characterized by an off-site production and its versatility of shapes, transported, and then bounded to the substrate employing a resin, primer, and putty. The pre-cured system can be

categorized as *pre-cured unidirectional laminate sheets*, *pre-cured multidirectional grids,* and *pre-cured shells.*

- *Near-surface-mounted (NSM) systems* or *surface-embedded NSM FRP systems*, this classification regards the use of circular or rectangular bars or plates placed into the groove where is bonded to the concrete surface. It is required an adhesive to bond the FRP material. This classification is divided into *round bars* and *rectangular bars and plates*.

2.3 Mechanical performance of FRP

The improvement of the structure's global performance relies on the combination of the enhancement of each element. Several types of research have studied the improvement of mechanical properties in structural elements; herein will be explicitly heading towards the noticeable effect of the increment in load capacity by confinement the structural elements, specifically, the columns.

2.3.1 Mechanical properties

Fiber and matrix mechanical properties can be extracted from fib (2006) and Monti and Petrone (2018), where the lower and upper threshold regarding the types are available, see Appendix A, Table 13. In Figure 1, FRP maximum strain is governed by the fiber ultimate strain, and the maximum stress is in-between the previously mentioned material's ultimate stress. A numerical example is depicted in Appendix A, Table 14.

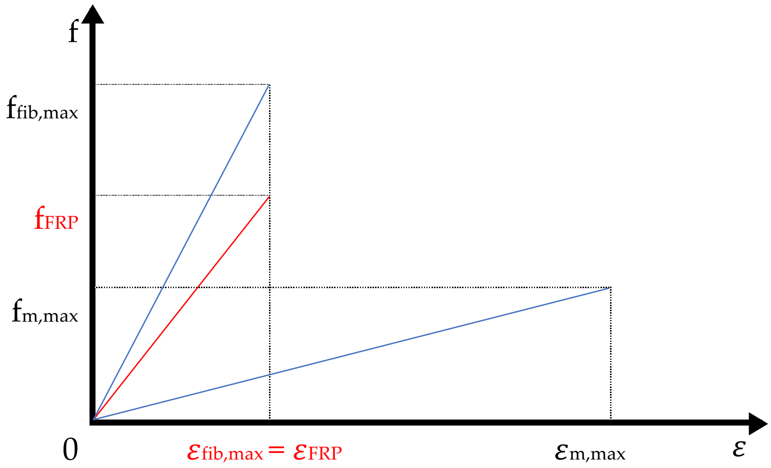

Figure 1 Stress-strain relationship of fiber, matrix, and FRP

2.3.2 Confinement effect in rectangular elements

FRP confinement effects have been investigated, and several strain-stress models were published (Ilki and Kumbasar 2003; Lam and Teng 2002; Lam and Teng 2003a; Lam and Teng 2003b; Spoelstra and Monti 1999). Based on experimental data, Ilki and Kumbasar (2003) were able to determine the effect of passive confinement given by FRP sheets in circular and non-circular columns that was implemented into fib (2006). In the present work, the design-oriented model developed by Lam and Teng (2003a) is used, which have been implemented in guidelines (e.g. ACI 2017); however, taking the modifications indicated in the design-oriented stress-strain model (Teng et al. 2009) by overcoming some deficiencies in their primary stress-strain model.

2.3.2.1 Stress-Strain model of FRP by Teng et al. (2009)

The confinement effect of FRP was modified to a more accurate expression, which considers a more precise reading of tensile rupture of FRP fiber and the descending branch (Teng et al. 2009). Therefore, three terms must be defined: the confinement ratio, which is taken from previous works f_l/f'_{co}, the stiffness ratio ρ_K and the strain ratio ρ_ε whose expression are depicted below:

$$\frac{f_l}{f'_{co}} = \frac{2E_{FRP}t\varepsilon_{h,rup}}{f'_{co}D} = \rho_K\rho_\varepsilon \tag{1}$$

$$\rho_K = \frac{2E_{FRP}t}{\left(\frac{f'_{co}}{\varepsilon_{co}}\right)D} \tag{2}$$

$$\rho_\varepsilon = \frac{\varepsilon_{h,rup}}{\varepsilon_{co}} \tag{3}$$

Where E_{FRP} and t represents the modulus of elasticity and thickness of FRP sheet, f'_{co} and ε_{co} is the unconfined concrete stress and strain and $\varepsilon_{h,rup}$ is the hoop ultimate strain. The confinement ratio, f_l/f'_{co}, is recommended to be greater than 0.07 (Lam and Teng 2003a; Spoelstra and Monti 1999). The equivalent diameter is herein calculated as Lam and Teng (2003b), which is depicted in Figure 2 and follows the expression:

$$D = \sqrt{b^2 + h^2} \tag{4}$$

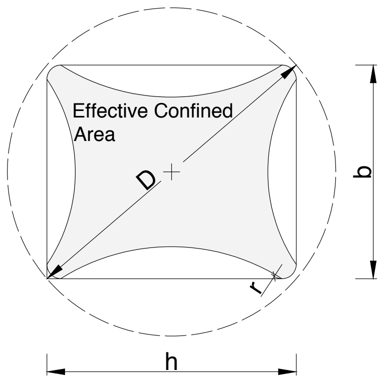

Figure 2 Equivalent rectangular cross-section diameter

The confined concrete strength, f'_{cc}, and the ultimate confined axial strain, ε_{cu}, is assessed following the below equations:

$$\frac{f'_{cc}}{f'_{co}} = \begin{cases} 1 + 3.5(p_K - 0.01)\rho_\varepsilon, & \rho_K \geq 0.01 \\ 1, & \rho_K < 0.01 \end{cases} \quad (5)$$

$$\frac{\varepsilon_{cu}}{\varepsilon_{co}} = 1.75 + 6.5\rho_K^{0.8}\rho_\varepsilon^{1.45} \quad (6)$$

The below expression summarizes the strain-stress relationship:

$$\sigma_c = \begin{cases} E_c\varepsilon_c - \dfrac{(E_c - E_2)^2}{4f'_{co}}\varepsilon_c^2, & for\ 0 \leq \varepsilon_c \leq \varepsilon_t \\ \begin{cases} f'_{co} + E_2\varepsilon_c, & if \quad \rho_K \geq 0.01 \\ f'_{co} - \dfrac{f'_{co} - f'_{cu}}{\varepsilon_{cu} - \varepsilon_{co}}(\varepsilon_c - \varepsilon_{co}), & if \quad \rho_K < 0.01 \end{cases} & for\ \varepsilon_t < \varepsilon_c \leq \varepsilon_{cu} \end{cases} \quad (7)$$

Where E_2 and ε_t are the second linear slope and the transition point, respectively, and are governed by the following expressions:

$$E_2 = \frac{f'_{cc} - f'_{co}}{\varepsilon_{cu}} \quad (8)$$

$$\varepsilon_t = \frac{2f'_{co}}{E_C - E_2} \quad (9)$$

A qualitative model the model is depicted in Figure 3.

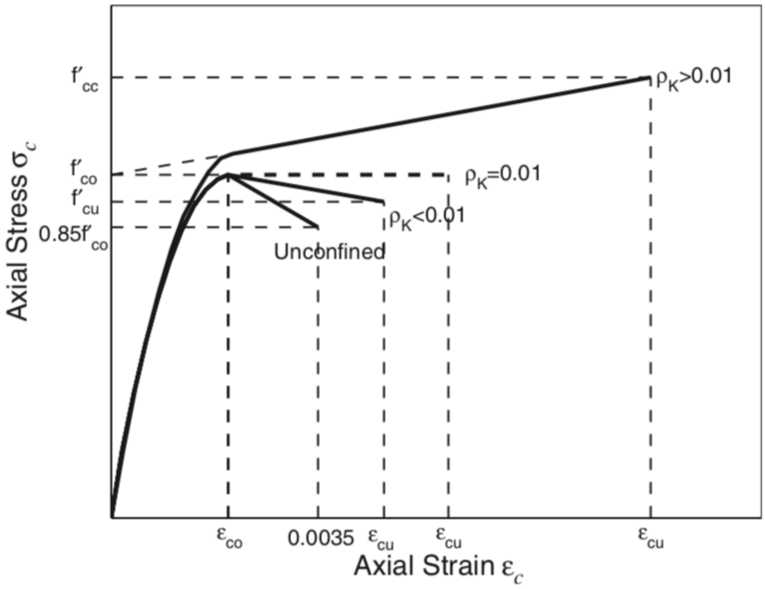

Figure 3 Qualitative stress - strain model (Teng et al. 2009)

2.4 Modes of failure of beam elements

Guidelines achieve to itemize each of the failure types that can be encounter by FRP retrofitting technique, as follow the first three modes are known to be classified within the *Ultimate Limit State* (ULS) criteria (ACI 2017):

a) Crushing of the concrete in compression before yielding of the steel reinforcement steel.
b) Yielding of the steel in tension before the rupture of FRP sheet.
c) Yielding of the steel in tension before the crushing of concrete.
d) Shear/tension delamination of the concrete cover.
e) Debonding of FRP from concrete substrate.

The failure *d* and *e* can be specified indicating the zone as (CNR 2013; fib 2001; fib 2006; Monti and Petrone 2018), see Figure 4:

- *Mode 1*: peeling-off in an uncracked anchorage zone.
- *Mode 2*: peeling-off caused at flexural zones.
- *Mode 3*: peeling-off caused at shear cracks.
- *Mode 4*: peeling-of caused by unevenness of the concrete surface.

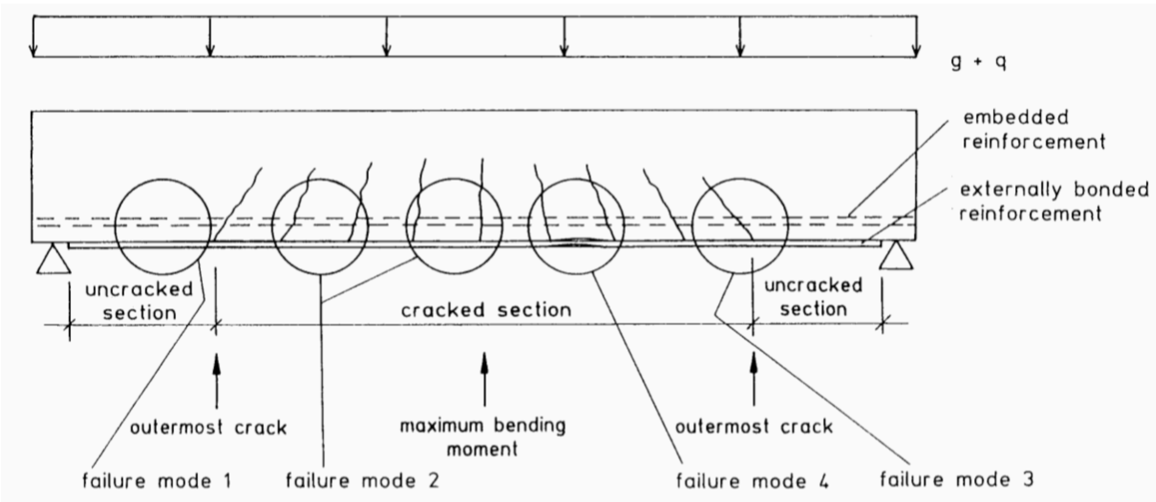

Figure 4 Bond failure modes of structural elements strengthen by FRP (fib 2001)

2.4.1 Column retrofitting by FRP

Standarized schemes have been implemented worldwide to overcome the previous mentioned mode of failures. Herein the jacketing of columns is applied to the elements to enhance the mechanical properties of each elements and improve the overall behavior of the structure. Guidelines depicts a diverse wrapping schemes for elements, see Figure 5. Despite the gamma presented in literature, the implemented layout of FRP wrapping chosen is an entire jacked and end-jacketing schemes, which from now on are called shear and moment confinement respectively, see Figure 6.

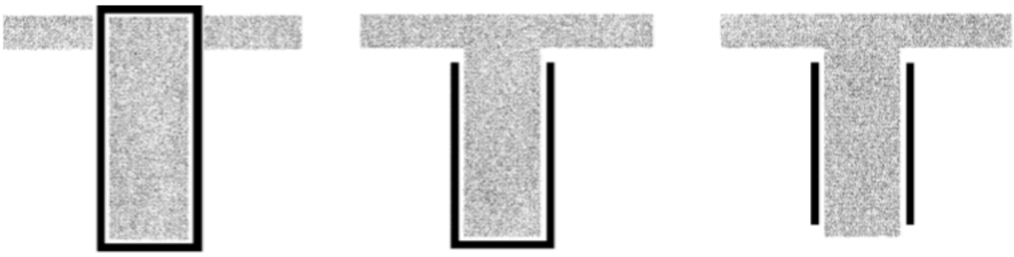

a) b) c)

Figure 5 FRP wrapped layout: a) four-sided or completetly wapped b) three-sided or U-wrapped c) two sided or bond-sided (ACI 2017)

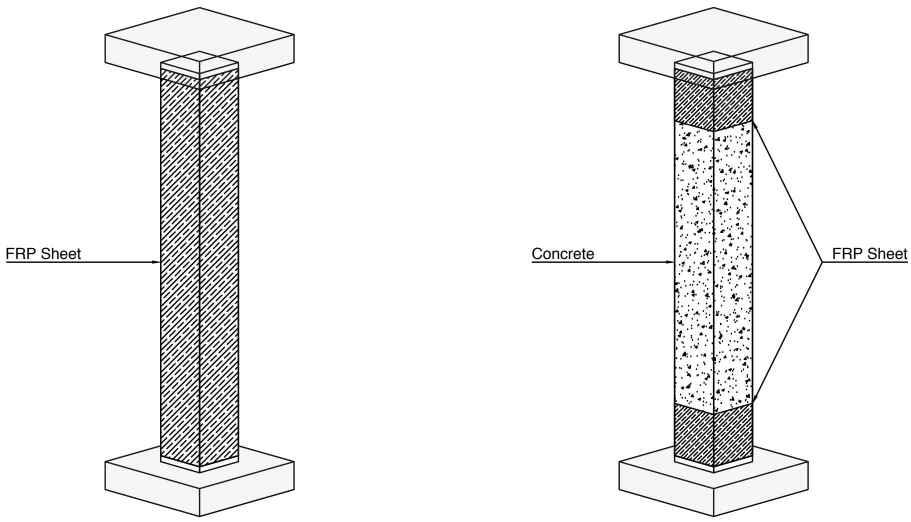

a) b)

Figure 6 Four-sided column FRP jacketing: a) shear confinement b) moment confinement

2.5 Joints strengthening by FRP

Beam-column joints are among the apex of the elements wich are required to have a deep detail to fulfil seismic demand. Nonetheless, historical and existing buildings are commonly characterize by nonforming detailing of nodes, leading to a poor seimic performance. Most guidelines does not mentioned RC joint strengthening with some exceptions (ACI 2017; CNR 2013). However, the application are left to researcher findings. Ilki et al. (2013) andPohoryles et al. (2019) briefly gathered information regarding the evaluated wrapping scheme of exterior nodes and failure modes of RC joints. Figure 7 depicts a simple example of a corner strengthened node.

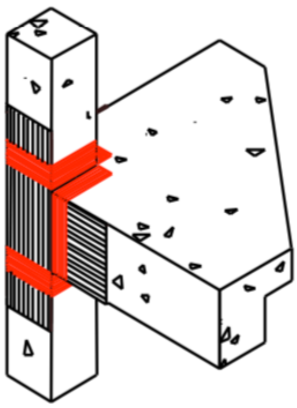

Figure 7 Exterior joint strengthenen by FRP sided wrapped (fib 2006)

2.5.1 Modes of failure of reinforced concrete joints

Six different joints failure can be categorize in RC frame structures when the expected joint capacity of the joint is lower than the adjacent elements (Ilki et al. 2013).

Table 1 Failure types of RC joints (Ilki et al. 2013)

Failure		Description of failure mode
1	J	Shear capacity of joint is reached
2	AJ	Longitudinal reinforcement of column presents buckling at joint level
3	BJ	Longitudinal reinforcement of beam yields and joint panel reaches shear capacity
4	CJ	Longitudinal reinforcement of column yields and joint panel reaches shear capacity
5	BCJ	Combination of previous two failures: BJ and CJ
6	SJ	Instability by poor anchorage of reinforcement leading to a decrement of shear capacity

The application of FRP strengthening of joints is used to avoid the previous failure modes and increase the shear capacity of joint panel. The expected failure mode after the strengthening is by yielding of the adjacent structural elements, with the expected strong column - weak beam behavior. Nonetheless, the FRP failure can occur as debounding or fracture of FRP sheets at the joint region (Ilki et al. 2013).

2.5.2 Shear capacity improved by FRP

Structural strengthening englobe the shear characteristics of the element, shear capacity can be improved by the application of FRP sheets around the element and guidelines cover the assessment of the increment as follow (ACI 2017; CNR 2013; EN8-3 2005):

$$V_{f,EC8} = 0.9 d f_{fe} 2 t_f \left(\frac{w_f}{s_f}\right)^2 (\cot\theta + \cot\beta)\sin\beta \;\; (for\ U - Shaped) \tag{10}$$

$$V_{f,EC8} = 0.9 d f_{fe} 2 t_f \left(\frac{w_f}{s_f}\right)\left(\frac{\sin\beta}{sin\theta}\right) \qquad (for\ two - sided) \tag{11}$$

$$V_{f,ACI} = 2 t_f f_{fe} (\sin\beta + \cos\beta)\, d_{fv} \frac{w_f}{s_f} \tag{12}$$

$$V_{f,CNR} = \frac{1}{\gamma_{Rd}}\ 0.9 d f_{fe} 2 t_f (\cot\theta + \cos\beta) \frac{w_f}{s_f} \tag{13}$$

ACI (American Concrete Institution) (2017) limits the maximum shear strengthening by FRP with the following equation:

$$V_s + V_f = 0.66\sqrt{f'_c}\, b_w d \tag{14}$$

Where V_s is the constribution of stirrups in shear.

Nonetheless, the following formulation is used to calculate the increment in shear by FRP sheets (Beydokhti and Shariatmadar 2016; Tsonos and Stylianidis 2002).

$$V_f = 0.9 t_f E_f \varepsilon_f d \cot\theta \tag{15}$$

In addition, Tsonos and Stylianidis (2002) determine the increment of compressive strength in joints by the confinement effect and is depicted in the following expression:

$$f_c = f_c' + 6\left(2a\frac{t_f}{D}f_{fd,c}\right)^{0.7} \tag{16}$$

Where $f_{fd,c}$ is expressed as $0.95f_{fk}$, which this latter is defined as the characteristic FRP strength. The thickness, t_f, and the equivalent diameter, D, which is evaluated as shown in Equation (17). The term depends on the geometry of the section and is evaluated as expressed in Equation (18).

$$D = \frac{b^2}{2h} + \frac{h^2}{2b} \tag{17}$$

$$a = 0.4 + 1.2\frac{R}{D} \tag{18}$$

Where R is the radius of rounded corners.

Following CNR (Council National Research) (2013) recommendation of limiting the tensile strain of FRP has been taken; hence, a maximum value of 0.4% is set.

Herein, the shear stress-strain backbone is set as defined by Hassan and Moehle (2012) with recommended values from De Risi et al. (2014) .A symmetric behavior is considered in the panel zone which is defined by four points: *cracking*, *pre-peak*, *peak shear strength* and *axial failure*. These points are assessed following below relationships:

- *Cracking point*

$$\tau_{j,1} = 0.29\sqrt{f_c}\sqrt{1 + 0.29\frac{P}{A_{j_f}}}\ (MPa) \tag{19}$$

$$\gamma_1 = 0.06\% \tag{20}$$

- *Pre-peak point*

$$\tau_{j,2} = 0.9\tau_{j,ps} \tag{21}$$

$$\gamma_2 = 0.26\% \tag{22}$$

- *Peak shear strength*

$$\tau_{j,3} = \frac{V_j}{A_j} \tag{23}$$

$$\gamma_3 = 0.63\% \tag{24}$$

- *Axial failure*

$$\tau_{j,4} = 0.7\tau_{j,3} \tag{25}$$

$$\gamma_4 = 0.03 \tag{26}$$

Where V_j and A_j are the shear strength and shear area of the panel zone. The initial joint shear modulus, G_{01} is calculated as 50% of the theoretical shear modulus $G_c = E_c/(1 + \nu)$. And finally, f_c is the compressive concrete strength and P the axial force.

2.6 Genetic algorithm optimization

Optimizing techniques have been an elderly task that brought the cooperation of several disciplines with a unique goal. The optimization problem can be found widely in any profession from social to scientific, and can be categorized depending on its scheme. A typical algorithm that has open a fan of solutions is the evolutionary-based algorithms that enter the meta-herustic algorithm classification. *Evolutionary-based Algorithm* or simply, *EA*, rose by following the same idea of survival of the fittest individual as Darwin's natural selection theory. Adeli and Sarma (2006) define *Genetic Algorithm* as:

> *"… a global search procedure for gradually improving the solution in succeeding populations using operations that mimic those of the natural evolution such as reproduction, crossover, and mutation and performs a random information exchange to create superior offsprings."*

The basis of finding an optimum value of a specific engineering problem regards the problem characteristic. *GA* is a metaheuristic algorithm which is defined as a global search within the domain problem. *GA* is directly juxtaposed to *Darwin's Evolution's Theory*, where a given population thrives by selecting, crossover, and mutating into new offsprings or children, see Figure 8a. The population is based on several individuals known as *chromosomes*, where each one of them has a probability of survival. A Binary population constitutes a simple genetic algorihm, see Figure 8b. A binary domain is the easiest approach in genetic algorithm, where each bit defines a specific property of the solution.

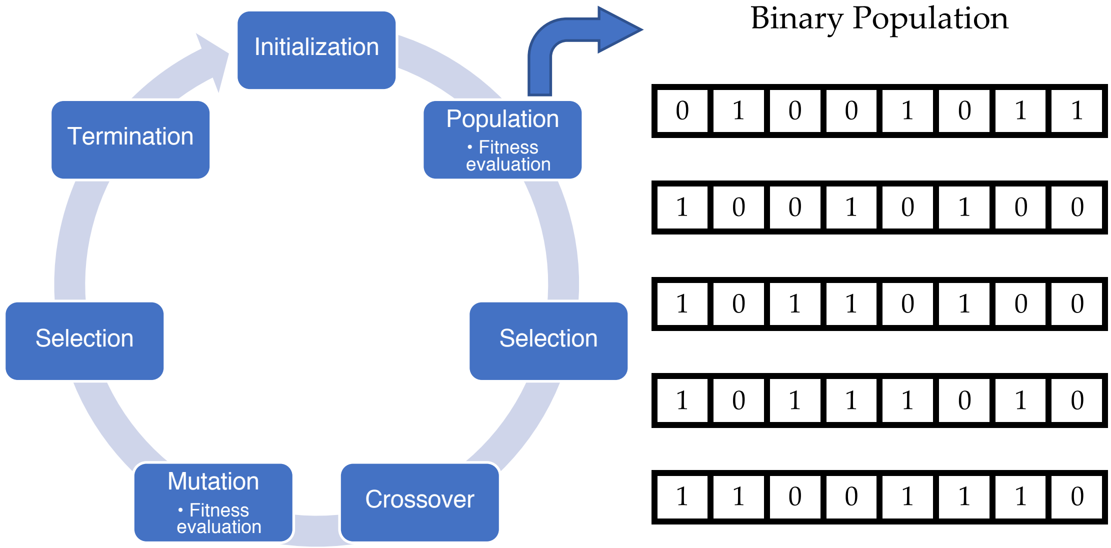

a) b)

Figure 8 Simple Genetic Algorithm: a) Loop of GA b) binary population

Genetic algorithm imitates the evolution of the real environment by simulating the phenotype changes, which define the chromosome's physical meaning. A real code environment will require more complex behavior in the individual's structure; however, this is left to the reader as it is not involved in the research's future development. In binary coding, genotype and phenotype take the same structure.

2.6.1 Genetic algorithm operators

Genetic algorithm optimization relies on the rate of crossover and mutation, which allows the exploitation of the solution domain. Therefore, for a given optimization problem, a different rate of these operators should be applied to improve the procedure's result.

2.6.1.1 Selection type

Selection, known as reproduction, is one of the essential aspects of genetic algorithm and follows a simple definition: selecting a set of individuals of the given population by its fitness value or survival probability (see Figure 9. This definition can simply be understood by copying and pasting gen to be in the new generation of offsprings (Adeli and Sarma 2006); therefore, this opens a wide window of possibilities in how the selection is performed, Kramer (2017) categorize selection as:

- *Comma selection*, this type of selection is characterized to select a number of best solutions of a given mating pool.
- *Plus selection*, following the same approach as *comma selection* but with a new feature picking the parents that share their genes to be in the new generation as their children.

- *Roulette wheel selection*, also known as *fitness proportional selection*, defines a mating pool where the selection is left to randomness depending on the fitness value.
- *Tournament selection*, as *Darwin's Evolution Theory*, a set of chromosomes is selected to contest for survival. The best individual in the competition will survive and inhere its genes to the new generation.
- *Elitism selection* sets a critical boundary on which chromosome is selected by being defined as a set of best individuals in the population to survive directly to the new generation.

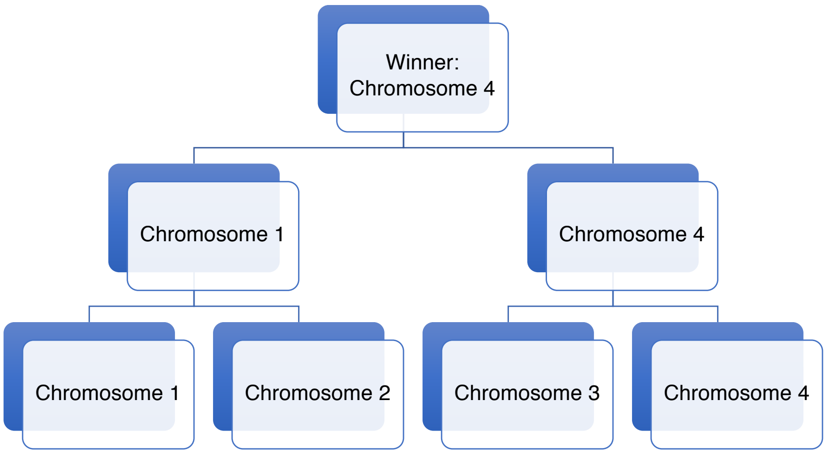

Figure 9 Tournament selection scheme

2.6.1.2 Crossover parameter

Crossover operator, as *selection parameter*, has a significant impact on genetic algorithm procedure. Crossover is defined by controlling how the selected chromosomes inhere their genes into the new population, see Figure 10. Several types of mixing have been developed. Herein will be discussed three of the most common:

- *Single point crossover* swaps the two parent chromosomes by fixing a pivot point, usually in the middle of the genes.
- *Double point crossover*, similar to the before-mentioned crossover, defines two points where the genes will be swapped; this commonly takes a symmetric splitting of the chromosome.
- *Uniform crossover*, a more random swapping takes place by merely defining the offsprings as having 50% of selecting a gen of the selected parents.

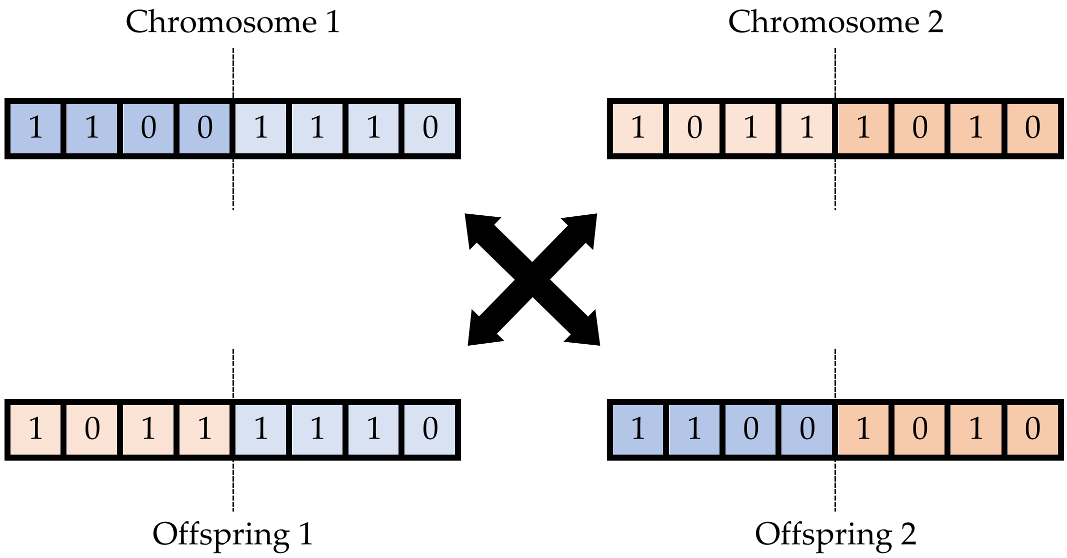

Figure 10 Single point crossover

2.6.1.3 Mutation parameter

Avoiding local optimum is one of the most challenging tasks when using a heuristic optimization tool. The introduction of mutation leads to an exhaustive global search in the domain of the problem by merely swapping the chromosome's random genes to avoid premature convergence. The mutation is characterized by being a unbiased parameter (Kramer 2017), which permits exploiting the domain of solutions. Adeli and Sarma (2006) define mutation operator as a safeguard in genetic algorithm that tries to imitate the real world evolution mutation by giving a small rate value.

Even of several studies in tunning parameters (Hassanat et al. 2019; Kucukkoc et al. 2013), tunning genetic algorithm procedures are time-consuming (Kramer 2017). Herein, Rechenberg 1/5th rule have been chosen to set the rate depending on the success by establishing a fix limit of 20%, the below pseudocode depicts the procedure Kramer (2017):

Table 2 Mutation rate pseudocode by Rechenberg Rule (Kramer (2017)

Rechenberg Rule: 1/5th
input:
measure success
if success rate > 1/5
increase mutation rate
elseif success rate ≤ 1/5
decrease mutation rate
end

2.6.2 Elitism and Memory-based GA

A most efficient algorithm has been recalled from setting a set of individuals that improve the optimization problem's convergence rate. *Elitism-based Genetic Algorithm* sets a new horizon in the evolutionary algorithm to avoid recurrent loss of optimal global solution or a fastest convergence into the solution (Kramer 2017). Herein, a set of elite members is saved in each iteration to further increase the beforementioned feature and reduce time consumption, the selection is made by a stochastic method which is mainly characterized by determine the best solution among the population in a given iteration.

Chapter 3

Optimal retrofitting strategy with Genetic Algorithm

The optimization procedure was implemented using the interaction between OPENSEES and MATLAB. The encouragement of the authors to use OPENSEES relies on its speediness in nonlinear analysis.

Material properties were input following researchers' indications and using the OPENSEES manual (Mazzoni et al.). Both confined and unconfined material were modeled using the *uniaxial Material concrete01*, which is defined by zero tensile strength. The confinement by FRP jacketing was implemented by using *uniaxial Material confinedConcrete01*, which is compatible with the before mentioned material as both cannot carry tensile strength. The reinforcement longitudinal reinforcement is integrated by using *uniaxial Material Steel02*, which contemplates a bilinear response.

3.1 Binary code implementation

The simple use of *binary coding* allows the clear identification of the required material within the genetic algorithm, as two retrofitted schemes are proposed plus the no retrofitted column, the use of two bits code for the columns is enough to identify the confinement of the element, see Figure 11.

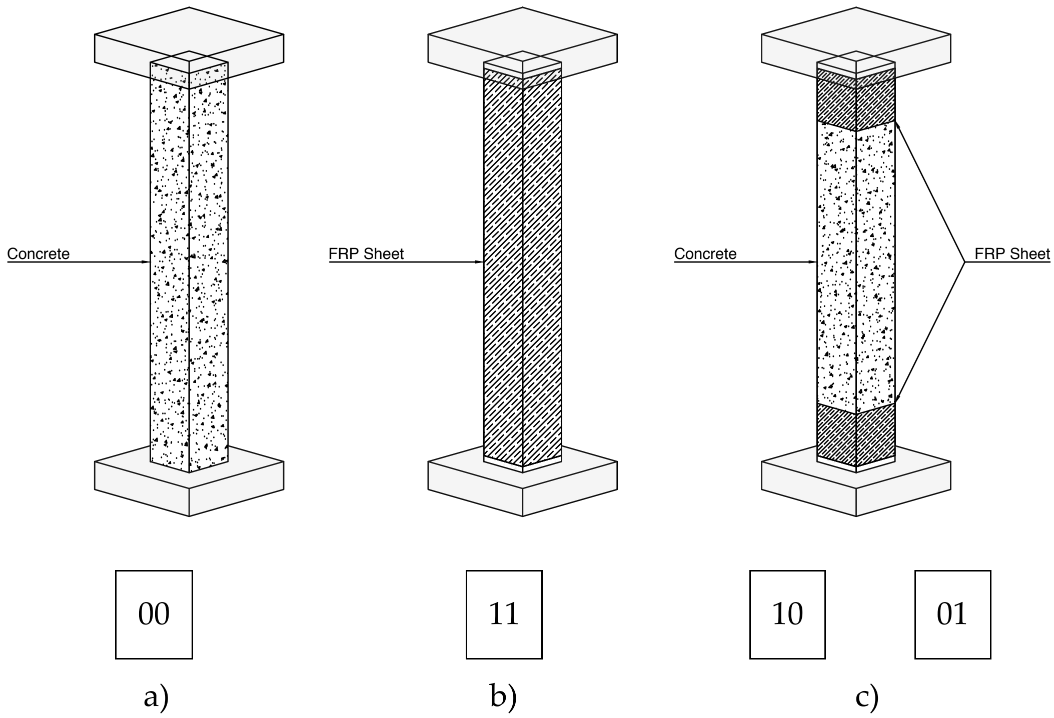

Figure 11 Binary coding implementation for retrofitted and non retrofitted columns: a) ties confinement (no retrofitted column) b) shear confinement c) moment confinement

The structural elements were model by using *forceBeamColum elements,* which define plastic hinges location by the setting integration points using a built-in feature known as *Integration HingeRadau* (Scott 2011). Pre-localizing the plastic hinge permits a higher speed in assessing the elements. The aforementioned plastic hinge location is assessed by using Priestley et al. (1996) formulation, as shown below:

$$L_p = g + 0.044 f_y d_{bl} \tag{27}$$

Where g represents the gap between the FRP sheet and intrados and extrados of the lower and upper story, guidelines recommend a value lower or equal to 5 cm (ACI 2017). The metaheuristic assessment is employed fixing the quantity of FRP sheets in the column, and this is done by verifying the requirements of the volumetric ratio of confinement, ρ_{FRP}, expressed by Priestley et al. (1996), which is depicted below:

$$\rho_{FRP} = 2nt\left(\frac{b+h}{bh}\right)\frac{w_{FRP}}{s_{FRP}} \geq \left(\frac{0.0052\rho_l D}{d_{bl}}\right)\frac{f_y}{f_{FRP}} \tag{28}$$

Where n is the number of sheets, b and h are the cross section dimension of the element, w_{FRP} and s_{FRP} are the FRP reinforcement ratio and spacement, respectively. D takes the value of the equivalent diameter given by Equation (17), ρ_l and d_{bl} are the longitudinal reinforcement ratio and the bigger diameter of the rebar; and finally, f_y and f_{FRP} are the yielding strength of the structural steel and FRP sheets.

Moreover, following the exposed arguments in Section 2.3.2.1 Equation (1), the granted enhancement criteria in confinement by FRP jacketing is verified.

The RC joints were implemented by using a binary codification, see Figure 12, paired with *Joint2D* in OPENSEES, this elements allows to consider the shear behavior of the panel with rotational spring surrounding the panel zone to represent the interface of the connected element, see Figure 13.

The implementation of the model is done by setting the rotational spring to fix end connection as the force based elements are set to represent a concentrated plasticity using Equation (27). The uniaxial material used to represent the shear behavior is *Pinching4*, and the cyclic response parameters have been set symmetrically according to Mitra and Lowes (2007), where *rDisp* is equal to 0.09, *rForce* is set to 0.21 and *uForce* is fixed to 0.0.

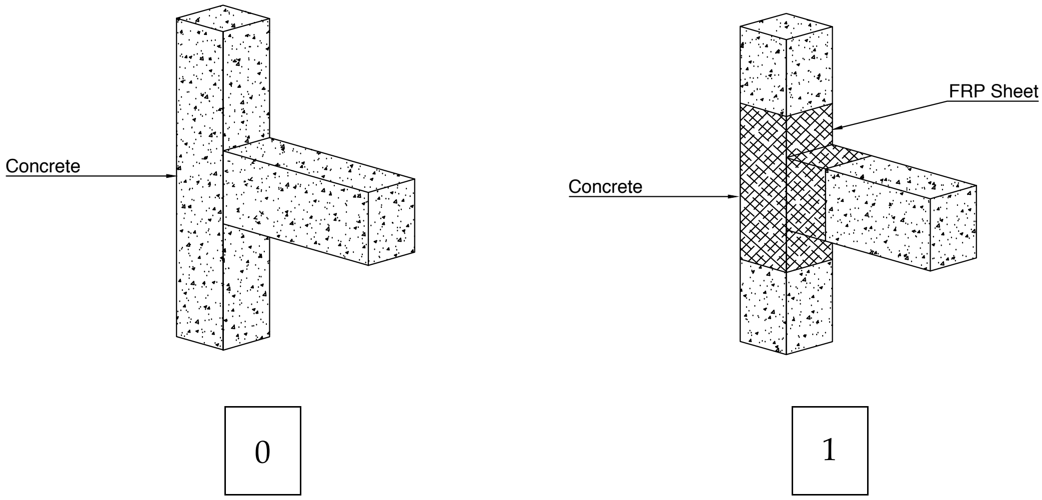

a) b)

Figure 12 Binary code implementation for non retrofitted and retrofitted joints: a) non retrofitted joint b) retrofitted joint

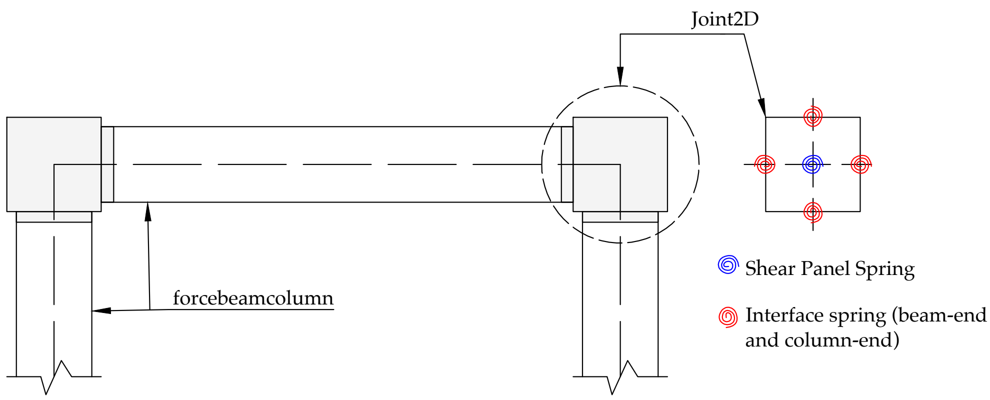

Figure 13 Simplify model integration of Joint2D

3.2 Evaluation of the fitness value of the individual

The population throve under the minimization problem criteria, and the fitness value is defined as the product of two parameters.

$$F = f_1 f_2 \tag{29}$$

The first term defines the square root of the sum of the square of the inter-story drifts (f_1), the second term is a penalty criterion that allows forcing a uniform drift along with the height. It is defined by taking into account the coefficient of variation of the inter-story drifts at each iteration concerning the non-retrofitted structure (f_2).

$$f_1 = \sqrt{\sum_{i=1}^{N} D_i^2} \tag{30}$$

$$f_2 = (1 + G)^2 \tag{31}$$

Where G is defined as shown in Equation (30), establishing the coefficient of variation, CoV, is defined as the ratio between the standard deviation, σ, and the mean value of the interstory drift, $\overline{D}$.

$$G = \frac{CoV_r}{CoV_o} \tag{32}$$

$$CoV = \frac{\sigma}{\overline{D}} \qquad \sigma = \sum_{i=1}^{N} (D_i - \overline{D})^2 \qquad \overline{D} = \sum_{i=1}^{N} D_i \tag{33}$$

Where the subscripts, r, and o, depict the retrofitted and original building structure, respectively. In addition, Equation (31) establishes the power of two, which allows increasing the constrain of this term within the objective function.

3.3 Flowchart of methodology

Genetic algorithm pseudocode is briefly depicted in the pseudocode shown in Figure 14, where it can be seen the iteration procedure in which the convergence takes place with recommended values for the input data, where the initial population is set to 5, the number of iterations is set to 5, the selection type is set fix to tournament, the crossover and mutation rate are 0.2 and 0.04 (following the 1/5th), respectively, and finally, the number of elite members is set to 1 or 2. The methodology of the implementation of the retrofitting strategy is depicted in Figure 15. Nonetheless, a preliminar assessment of the structure is required as the coefficient of variation, given by Equation (31), is used to determine the uniformity of interstory drift.

```
Genetic Algorithm
input:
        p_m: population
        iter: max generation
        s: selection control
        c: crossover rate
        m: mutate rate
        el: number of elite members
output:
        initialize p_m
        evaluation of individuals (c)
        initialize el_m
        for i = 1:iter
            p_i: select parents
            offprings: crossover(p_i)
            offprings: mutate(p_i)
            evaluate offprings
            update mutation rate (1/5th rule)
            elites: update elite members el_m
        end
end
```

Figure 14 Pseudocode of Genetic Algorithm

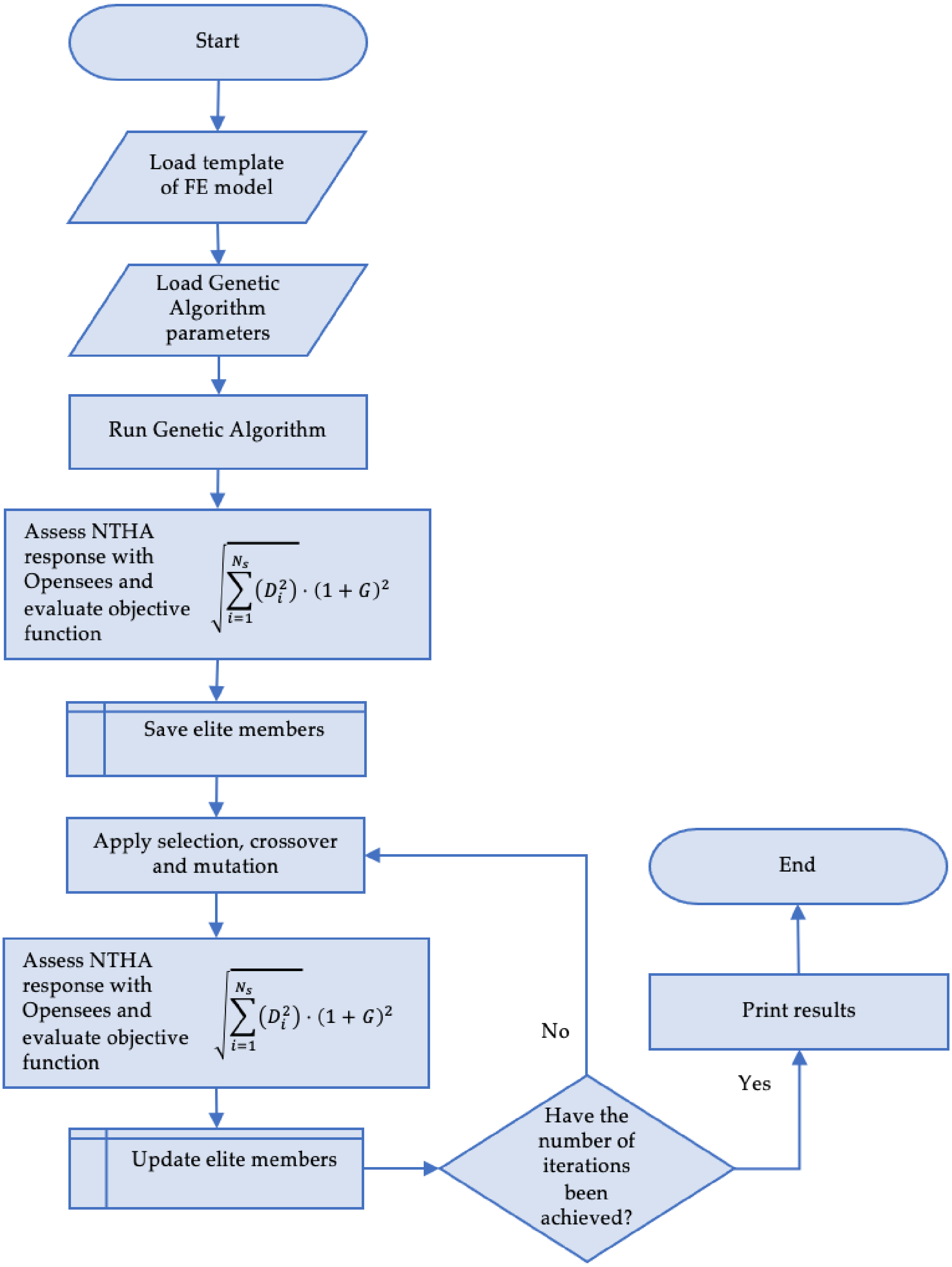

Figure 15 Flowchart of optimal retrofitting strategy

Chapter 4

Assessment Of Space Frame Structure

4.1 Case study A: Space frame RC building structure

A space frame reinforced concrete structure is chosen to be tested and to further develop the methodology of the retrofitting strategy. Therefore, the building structure requires to be assessed and to verify its seismic performance. The assessment is realized by taking into account the Italian regulations (NTC 2018) and European Standards (EN 2005), where the latter establishes the formulation for the initial modulus of elasticity as a percentage of the secant relationship, which is expressed below, the mechanical properties employed in the model are depicted Table 3.

$$E_{cm} = 22000\left(\frac{f_{ck} + 8}{10}\right)^{0.3} \tag{34}$$

The RC space frame structure is a symmetric building with equal dimensions in both directions and presents a regularity in plan and height; see Figure 18a,b. Structural elements present a volumetric longitudinal reinforcement, ρ_l, equal to

0.015 for each column and 0.0065; both with a transversal reinforcement of 8 mm reinforcement with a spacing of 200 mm as depicted in each cross-section, see Figure 18c,d. Furthermore, a tag identification for each of the column is shown in Figure 17.

Table 3 Material properties of Case study A: a) unconfined concrete b) structural steel

Concrete		
f_c	25	*MPa*
E_c	31475	*MPa*
η	0.2	~
G	13115	*MPa*

a)

Steel		
f_y	450	*MPa*
E_s	210000	*MPa*
η	0.3	~
G	80769	*MPa*

b)

Seeting the properties of FRP as a young modulus of 530 GPa and tensile strength of 2100 MPa, leading to a strain of approximately 0.4%, the obtained stress-strain relationship is shown in Figure 16 by using Teng et al. (2009) formulation.

The implementation of the retrofitting strategy for case A was realized by setting as input ground motion a single record to further explore the genetic algorithm parameters as shown in Section 3.3.

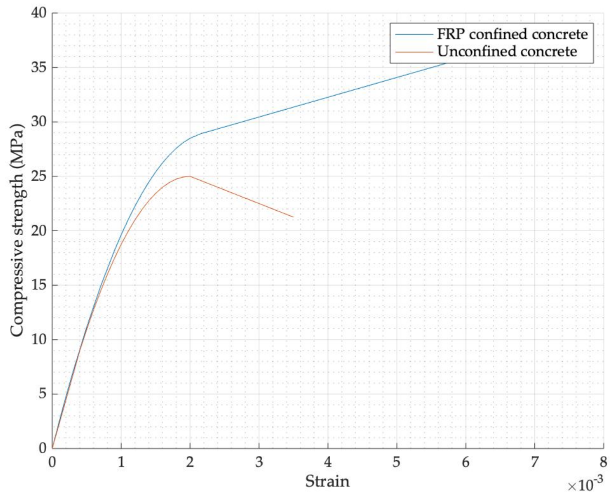

Figure 16 FRP confined concrete and unconfined concrete of case A

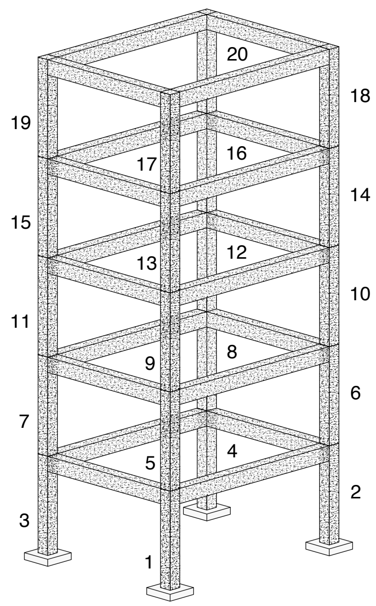

Figure 17 ID of columns of the case study A multistory RC building structure

The structure is lozalized at L'Aquila, center of Italy, with the followings coordinates: lat: 42.3849, lon: 13.3548, with an ID: 26305 given by Istituto Nazionale di Geofisica e Vulcanologia (INGV) (2007).

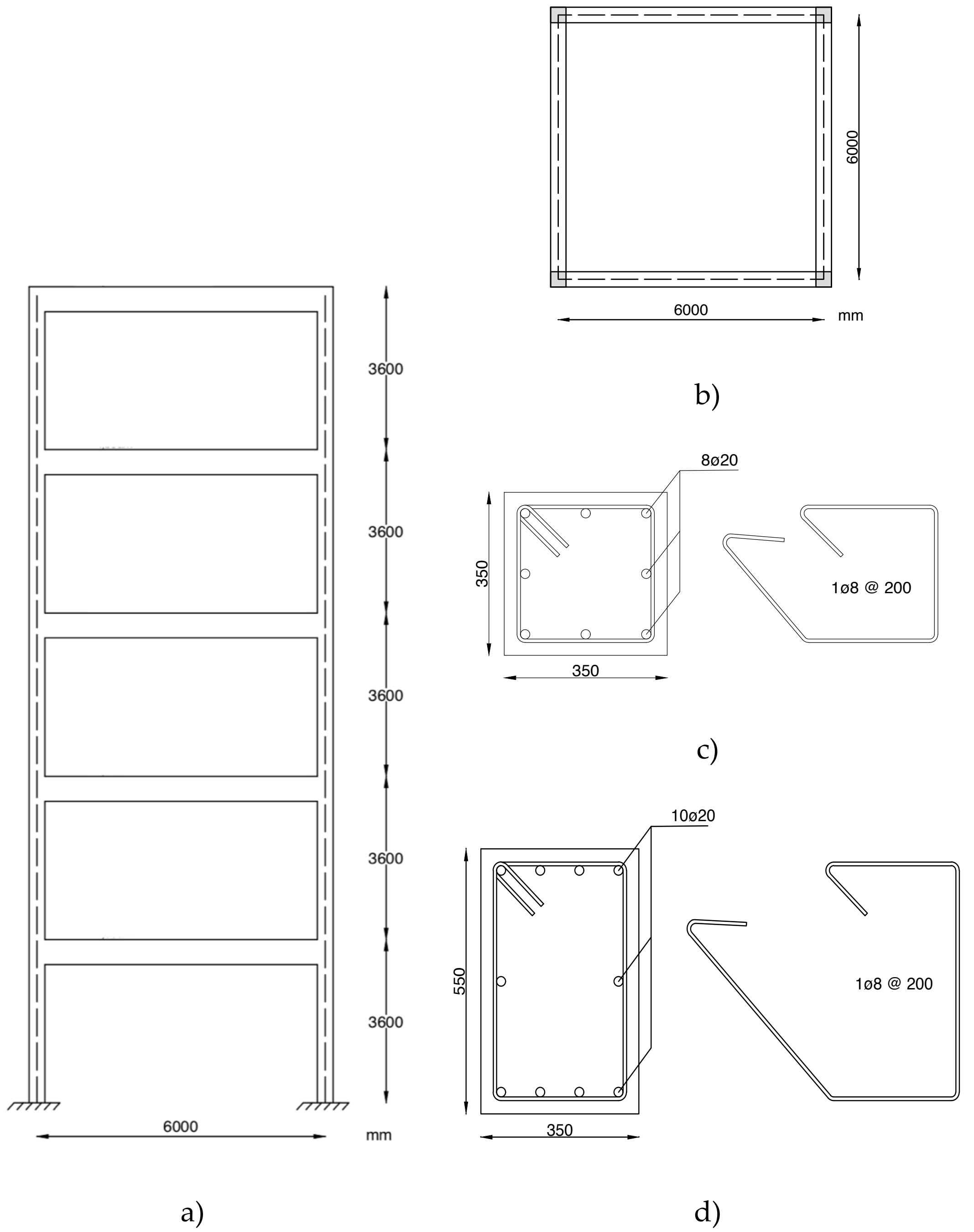

Figure 18 Case study: a) view of frame X (same as frame Y) b) Plan view c) column cross-section d) beam and girder cross-section

4.1.1 Seismic parameters of the territory

The Italian guideline (NTC 2018) establishes the seismic features of the Italian territory. For the case study, L'Aquila earthquake has been set to have for a return period (T_r) of 405 years, a peak acceleration (a_g) of 2.606, a maximum spectral amplification (F_0) of 2.36 and an initial of the constant velocity branch (T_C^*) (with dependence on the type of soil, C_C) of 0.35. The use of OPENSIGNAL Cimellaro and Marasco (2015) allowed the proper introduction of the parameters and the Elastic Design Spectrum data extraction, see Figure 19a. The introduction of the *ADRS* format is realized by assessing the pseudo displacement, S_d, see Equation (35).

$$S_d = \frac{T^2}{4\pi^2} a_g \tag{35}$$

Where T depicts the spectrum's period, the application of the previous equation yields the plot shown in Figure 19b.

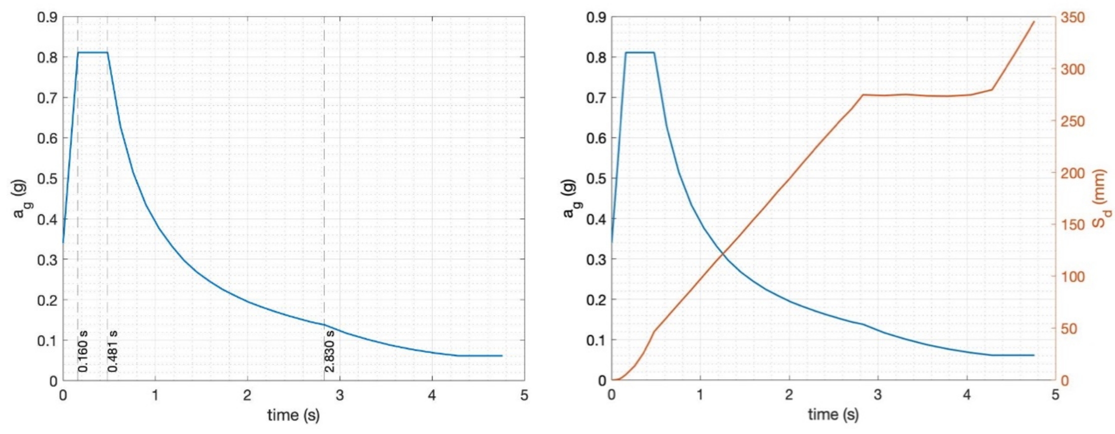

a) b)

Figure 19 Response Spectrum of L'Aquila territory: a) Design Response Spectrum b) Acceleration Displacement Response Spectrum (ADRS) format

4.1.2 Ductility capacity evaluation

The space fram RC structure assessment was done through a pushover analysis following the Italian criteria (NTC 2018) where the load case is defined by Equation (36). Which takes into account permanent structural and non-structural loads, G_1 and G_2, and the quasi permanent loads, where ψ_{2j} is equal to 0.3, defining a residential use.

$$G_1 + G_2 + \sum_j \psi_{2j} Q_{kj} \tag{36}$$

The assessment was realized by modeling the structure in SeismoStruct, the model is constituted by lumped masses in the nodes and distributed plasticity elements. The software's built-in features allow to realize the evaluation the target displacement following the previously mentioned Italian regulation. The pushover analysis result of interest, the capacity curve, is shown in Figure 20, where the drop of the lateral strength by a 15% is found at a 244 mm top displacement. Besides, as stated in the regulation, the idealized bilinear capacity curve is assumed to have an initial stiffness equal to the 60% of the yield strength.

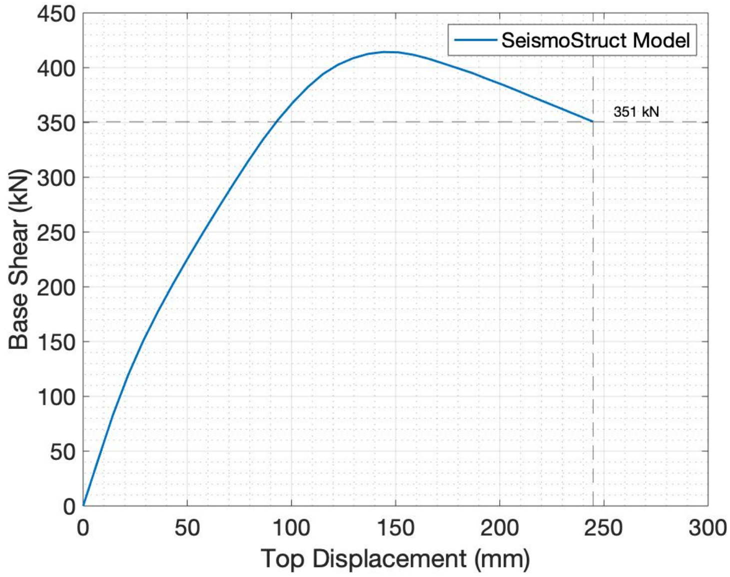

Figure 20 Capacity curve with SeismoStruct

The transformation of the multi-degree of freedom system (*MDFs*) into a single degree of freedom system (*SDFs*) is found by assessing T^* with the below equation:

$$T^* = 2\pi\sqrt{\frac{m^*}{K^*}} \tag{37}$$

Where m^* and K^* are the mass associated to the first modal participation factor and the stiffness of the bilinear capacity curve.

$$m^* = \sum m_1 \phi_1 \quad (38)$$

The conversion into a SDFs is therefore developed by dividing the capacity curve parameters by the first modal participation factor, Γ_1, which is evaluated using the following expression. Figure 21 depicts the comparison between the idealized bilinear curve of both MDFs and SDFs.

$$\Gamma_1 = \frac{\sum m_1 \phi_1}{\sum_{i=1}^{n} m_1 \phi_1} \quad (39)$$

Finally, the ductility assessment considers the inelastic design spectrum, which is calculated by employing the constant ductility factor, μ. This parameter is evaluated through the reduction factor, R_μ, which is assessed with the following formulation:

$$R_\mu = \frac{S_{ae}}{S_{ay}} \quad (40)$$

Where S_{ae} and S_{ay} the elastic and inelastic acceleration demand of the system. The application of the previously mentioned equation yields the results depicted in Table 4.

Table 4 Results of ductility demand evaluation

SDF parameters	
Mass, m^{*} (T)	549.8
Period, T^{*} (s)	2.23
Stiffness, K^{*} (kN/m)	4362
Modal participation factor, Γ_1	1.321
Reduction factor, R_μ	3.19

A graphical evaluation allows the visual verification of the results as is shown in Figure 22, where the structure cannot undergo the required displacement demanded by the seismic motion.

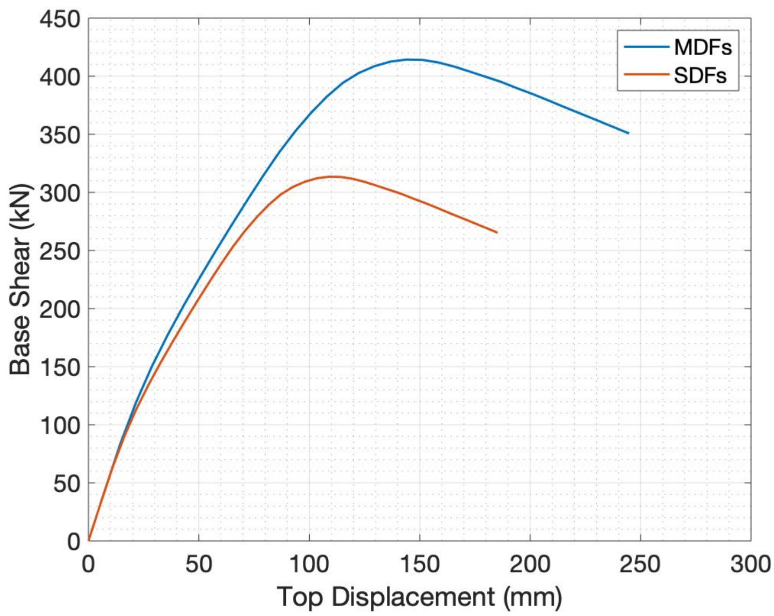

Figure 21 Juxtaposition of capacity curve of the MDFs and SDFs of the case of study

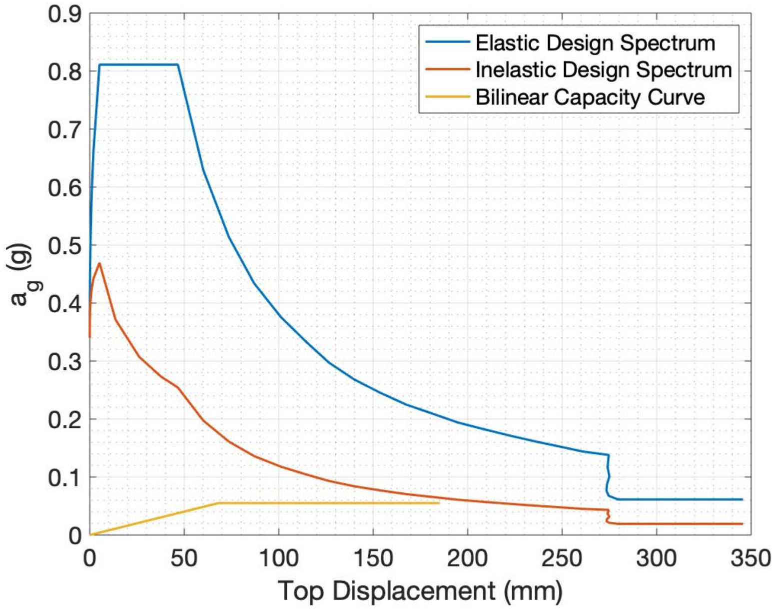

Figure 22 Ductility demand verification in ADRS format

4.2 Case study B: Archetype models of California's building structures

A set of space frame structures are chosen to verify the applicability of the methodology. The chocen RC frame are commonly California's existing office building built in the late's 60-70s characterized to be non ductile structures (Liel 2008). Archetype models were developed to further englobe the behavior of existing buildings in the zone where the mechanical properties of material are shown in Table 5. The selected archetype models are a 4 and 12 story building. Particularly, the properties regarding the structural elements of the 4 story building are defined in Table 6 and Table 7. In the case of the 12 story building, the geometry and properties of structural elements are shown in Table 8 and Table 9 with slight variation with respect to those shown in the dissertation of the previous mentioned author.

Table 5 Material properties of Case study B: a) unconfined concrete b) structural steel

Concrete		
f_c	27	MPa
E_c	32036	MPa
η	0.2	~
G	13348	MPa

a)

Steel		
f_y	400	MPa
E_s	210000	MPa
η	0.3	~
G	80769	MPa

b)

Applying the same approach as case A, the FRP properties input with the previous declared concrete mechanical properties, the stress-strain relationship is shown in Figure 23.

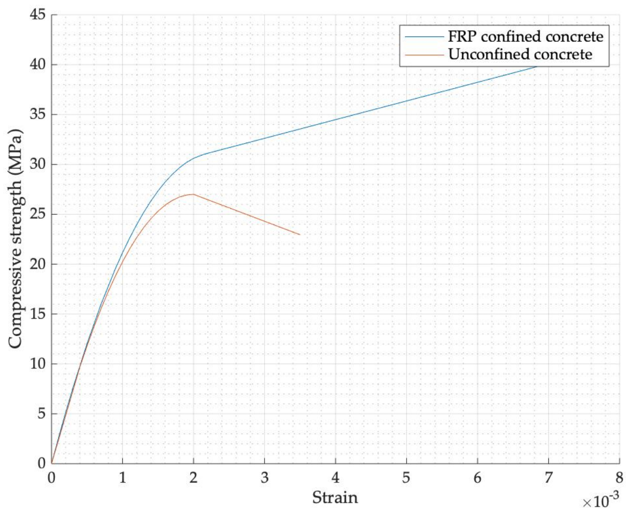

Figure 23 FRP confined concrete and unconfined concrete of case B

Table 6 Column properties of 4 Story Space frame structure

Column ID	Geometry		Mechanical properties of element	
	h (mm)	b (mm)	ρ_L (-)	ρ_{sh} (-)
C1	500	500	0.0393	0.0039
C2	500	500	0.0289	0.0028
C3	500	500	0.0289	0.0022
C4	500	500	0.0193	0.0015
C5	500	500	0.0122	0.0022

Table 7 Beam properties of 4 Story Space frame structure

Beam ID	Geometry		Mechanical Properties		
	h (mm)	b (mm)	ρ (-)	ρ' (-)	ρ_{sh} (-)
B1	660	660	0.0075	0.0117	0.0021
B2	660	660	0.0066	0.0117	0.0021
B3	500	500	0.0012	0.0199	0.0021
B4	500	500	0.0012	0.0199	0.0021

Table 8 Column properties of 12 Story Space frame structure

Column ID	Geometry		Mechanical properties of element	
	h (mm)	b (mm)	ρ_L (-)	ρ_{sh} (-)
C1	660	660	0.0412	0.0060
C2	660	660	0.0231	0.0068
C3	660	660	0.0231	0.0045
C4	660	660	0.0231	0.0060
C5	660	660	0.0202	0.0040
C6	660	660	0.0231	0.0060
C7	660	660	0.0137	0.0015
C8	660	660	0.0137	0.0030
C9	660	660	0.0126	0.0015
C10	660	660	0.0106	0.0015

Table 9 Beam properties of 12 Story Space frame structure

Beam ID	Geometry		Mechanical Properties		
	h (mm)	b (mm)	ρ (-)	ρ' (-)	ρ_{sh} (-)
B1	800	660	0.0057	0.0110	0.0021
B2	800	660	0.0050	0.0110	0.0021
B3	800	660	0.0047	0.0110	0.0021
B4	800	660	0.0047	0.0110	0.0021
B5	800	660	0.0047	0.0110	0.0021
B6	800	660	0.0047	0.0135	0.0021
B7	660	660	0.0050	0.0135	0.0020
B8	660	660	0.0050	0.0124	0.0020
B9	660	660	0.0050	0.0113	0.0020
B10	660	660	0.0050	0.0087	0.0020
B11	660	660	0.0050	0.0061	0.0020
B12	660	660	0.0050	0.0106	0.0020

The analysis have been carried out by assessing the structure as depicted in Figure 24 and Figure 25, where the length of each bay is 7600 mm (L_{bay}) and the first story (H_1) and other stories height (H_N), are 4600 and 4000 mm, respectively. In addition, variation in some stories have been made to model height irregularities, specifying an increment of 30% of the interstory height in floor 5, 9 and 12. Herein, the 4 RC story building is depicted as case B1, and the 12 RC building and the modified structure are case B2 and B3. The modal analysis of the each structure yields a fundamental period 0.96 s, 2.00 s and 2.15 s for B1, B2 and B3, respectively, which is considerably higher than the established by codes. Particularly, as the code established an approximate equation for structures up to 40 m, the case B1 yields a fundamental period of 0.62 s; however, this increment is addressed to the consideration of panel zones in joints which adds an certain extend of flexibility to the structures.

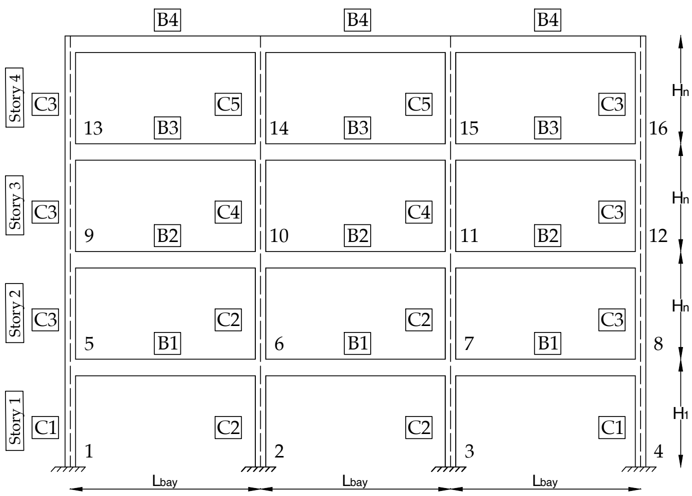

Figure 24 Identification of structural elements in 4 story space frame structure and tag ID of columns

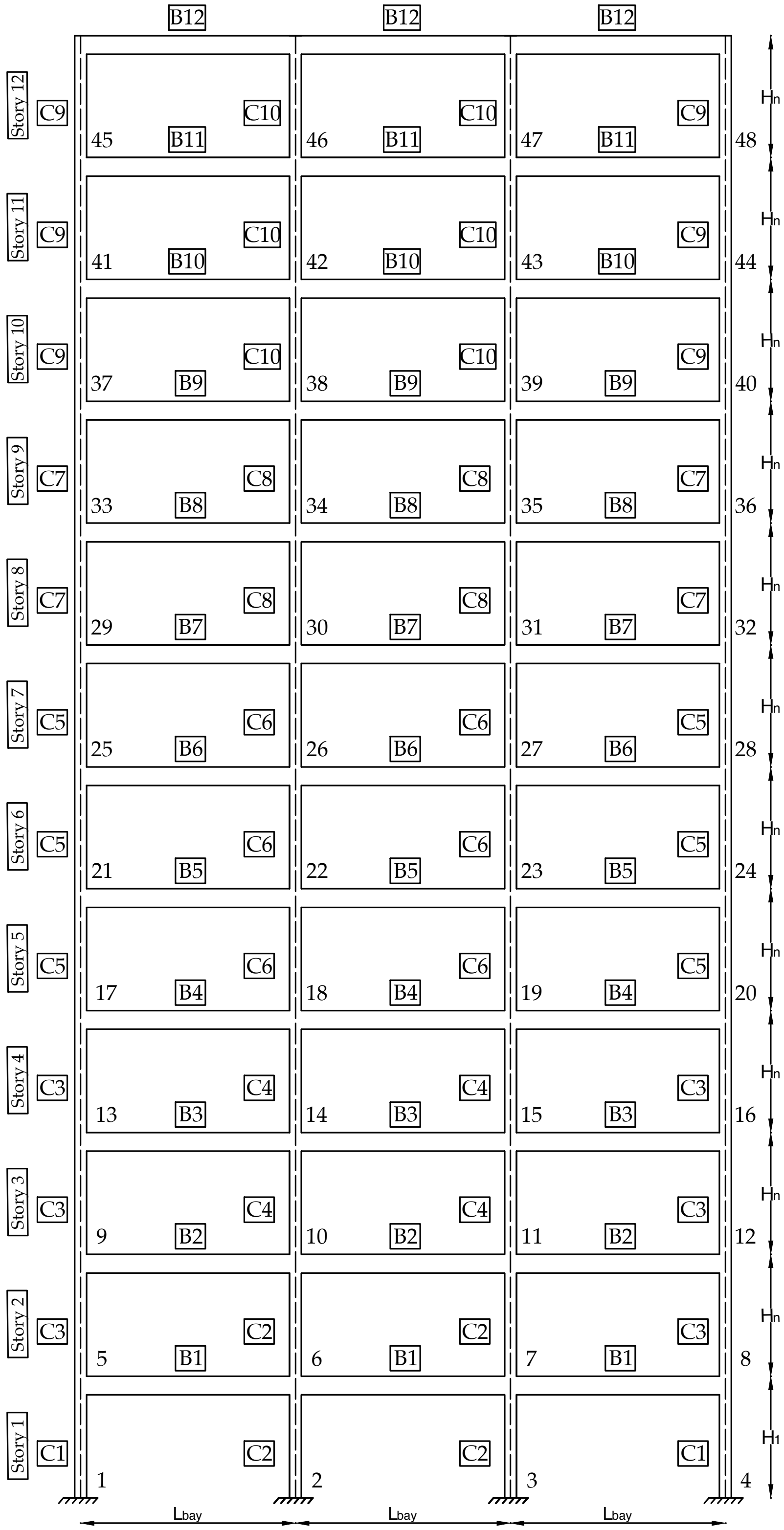

Figure 25 Identification of structural elements in 12 story space frame structure and tag ID of columns

4.2.1 Seismic parameters of California territory

ASCE (American Society of Civil Engineers) (2017) establishes the seismic mapped parameters according to the location in the United States of America. For the specific case of California, the design/inelastic response spectrum is defined with S_S equal to 1.5 and S_1 equal to 0.6, with a transition period T_L set to 8.0 seconds, see Figure 26.

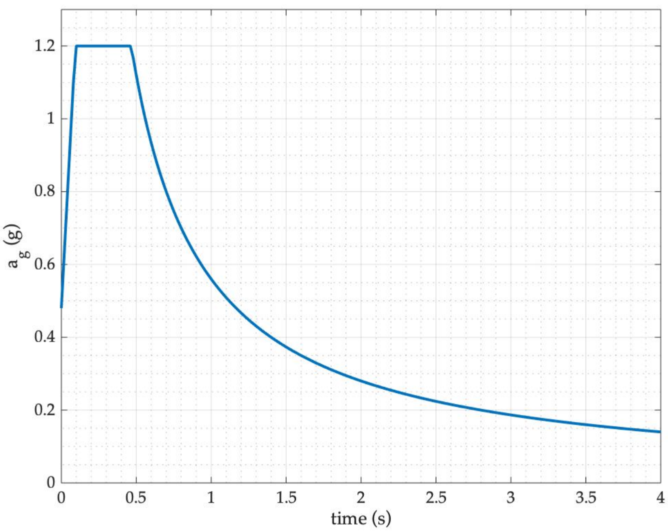

Figure 26 Design/inelastic response spectrum of California

The assessment is realized by selecting a set of Time - History for the evaluation of NLTH. For case study B, a set of 10 records is selected and matched according to EN (European Committee for Standardization) (2005), see Table 10. where the minimum and maximum bounds of fundamental period for matching each record is $0.2T$ and $1.5T$ as established by guidelines . The selection and scaling procedure have been done by employing SeismoSelect and SeismoMatch softwares. The selection of ground motion is mainly focus on the comparison of the applicability of the strategy wih Near-Fault and Far-Fault events. The ground motion has been coded as *GMijz*, where *i* is 1 or 2 defining Far-Fault or Near-Faul, respectively; *j* represents an unique tag for each seismic event and *z* depicts the component which takes the value 1 or 2 and it is used in Section 4.3.

Table 10 Set of Time - History records selected from NGA Strong Ground Motion Database (PEER 2014)

Ground Motion	Event Name	Year	Type	Magnitude	Code
Far-Fault	Cape Mendocino	1992	Reverse	7.01	GM12
	Northridge-01	1994	Reverse	6.69	GM14
	Landers	1992	Strike Slip	7.28	GM15
	Superstition Hills-02	1987	Strike Slip	6.54	GM17
	Northridge-01	1994	Reverse	6.69	GM18
Near-Fault	N. Palm Springs	1986	Reverse oblique	6.06	GM23
	Erzican, Turkey	1992	Strike slip	6.69	GM24
	Parkfield-02, CA	2004	Strike slip	6.00	GM25
	Christchurch, New Zealand	2011	Reverse oblique	6.20	GM26
	Zealand	2011	Reverse oblique	6.20	GM27

4.3 Algorithm output analysis

4.3.1 Results of case study A

The RC building structure is assessed by realizing the before mentioned flowchart an evaluating the different layout for the FRP jacketing in columns. The implementation of the joints strengthening is left to case study B as the inclusion of more nodes is required to develop a more refine finite element model.

The implementation of the strategy yields an convergence to an optimum value within a given range which as been set to a number of 50 iteration. By analyzing the possible layout scheme in each modified finite element model, three cases are presented herein by change a single parameter, the number of elite members storage in the genetic algorithm.

The three cases are 0, 1 and 2 elite members. The first two results, Figure 27 and Figure 28, depicts the terms within the objective function evaluated in the metaheuristic approach, see Figure 29, where the convergence to an optimum value is found in each case; nonetheless, by implementing a pair of elite members, a more uniform drift or a lower coefficient of variation is encounter by juxtaposed both cases, the use of no elite member and the input of two set of these, see Figure 30a,c.

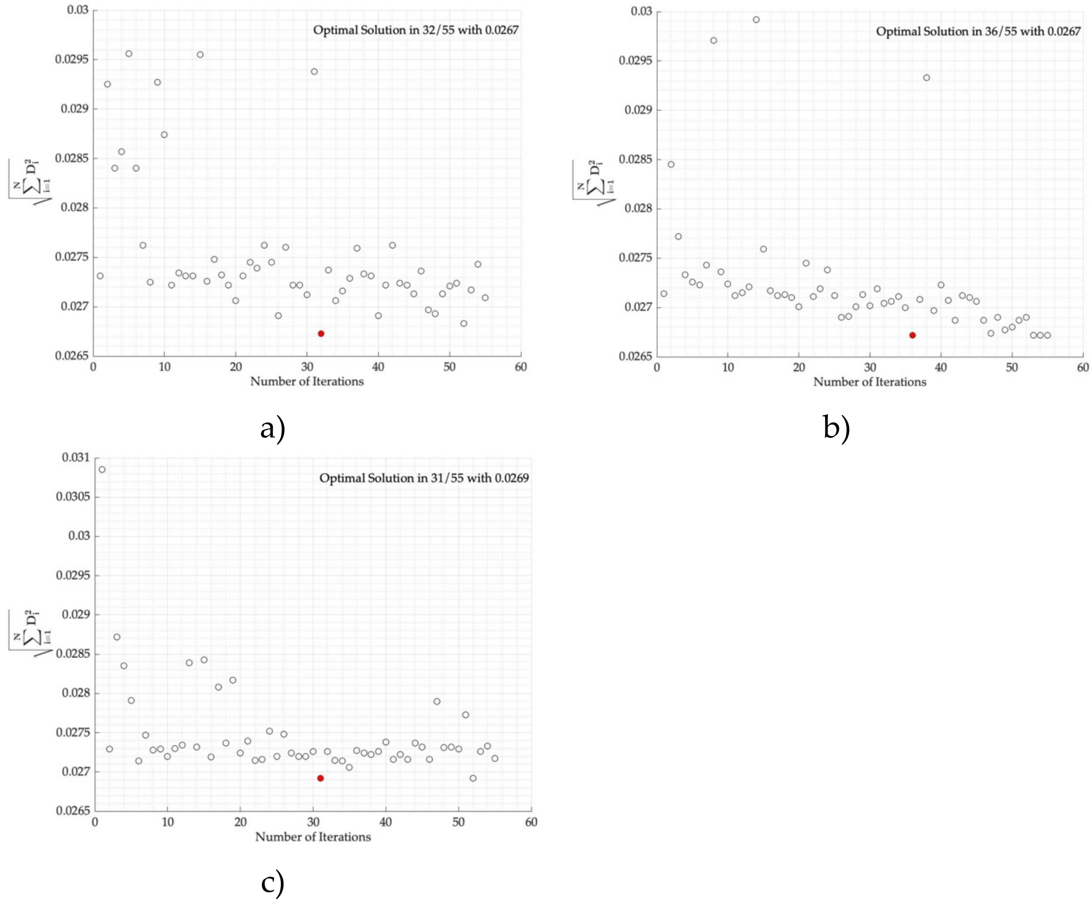

Figure 27 Results main function f_1 for case study A: a) no elite member b) one elite member c) two elite members

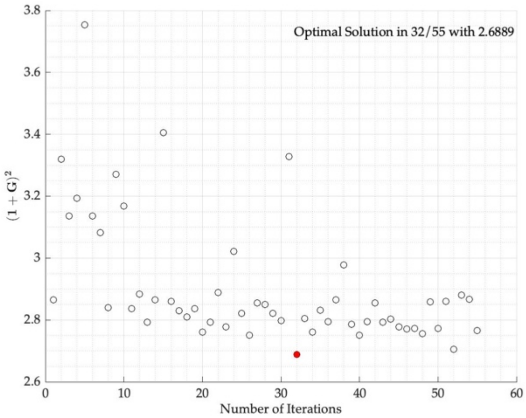

a)

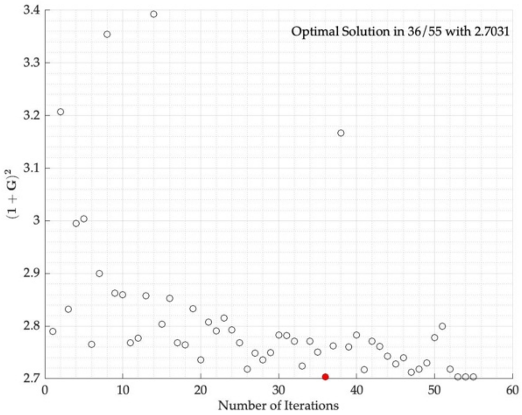

b)

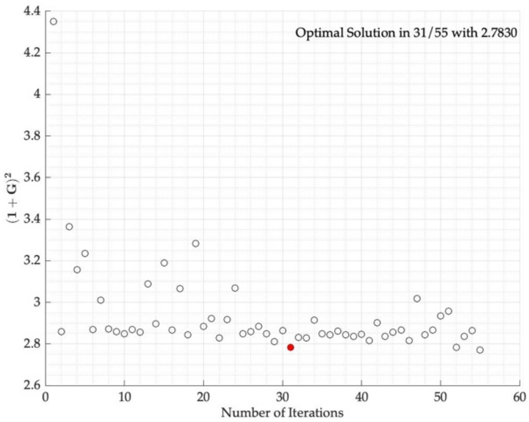

c)

Figure 28 Results of penalty function f_2 for case study A: a) no elite member b) one elite member c) two elite members

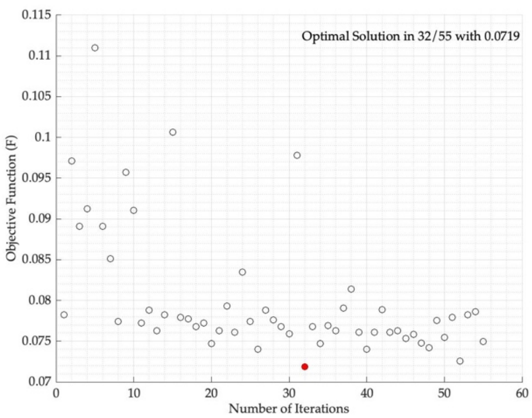

a)

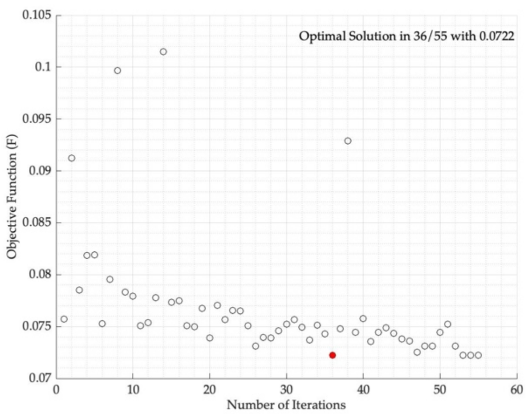

b)

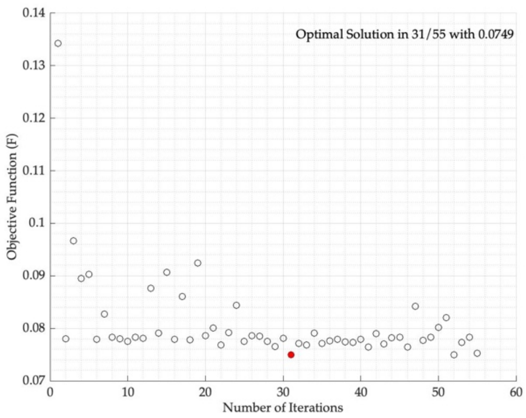

c)

Figure 29 Results of objective function F for case study A: a) no elite member b) one elite member c) two elite members

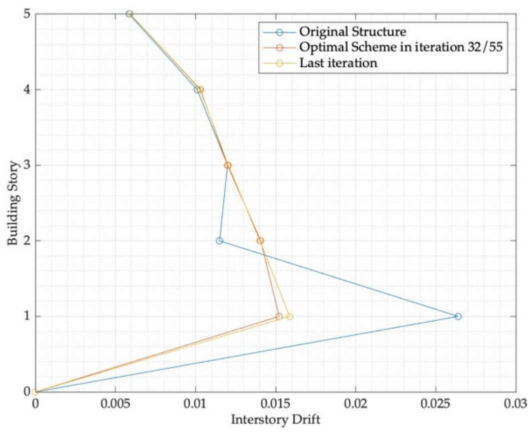

a)

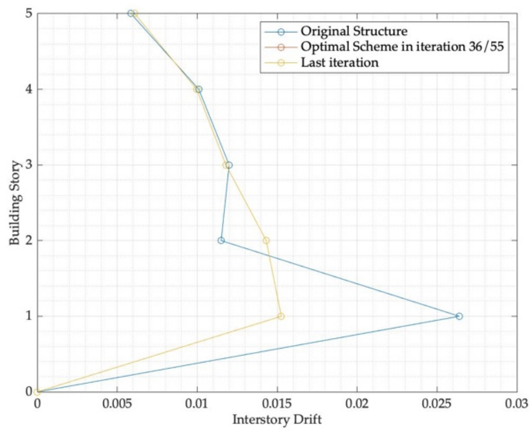

b)

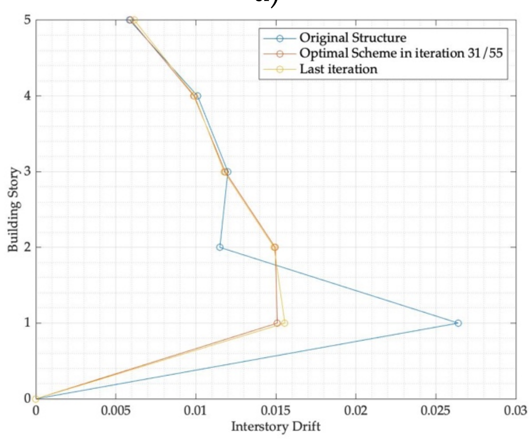

c)

Figure 30 Interstory drift for case study A: a) no elite member b) one elite member c) two elite members

The usage of FRP jacketing in columns is found to be expected, for this particular case, in the lower stories of the building where the interstory drift is higher . This probability increases with the consideration of elite members in the input data of the genetic algorithm, see Figure 31b,c. This effect can be seen clearly by the juxtaposition of the material usage in the first story of the RC frame, see Figure 32. The percentage of material is considered to be 0%, 27% and 100% for unretrofitted column, moment confinement and shear confinement, respectively. The percentage is assessed according to the length of the wrapped column as the rest of the parameters are fixed.

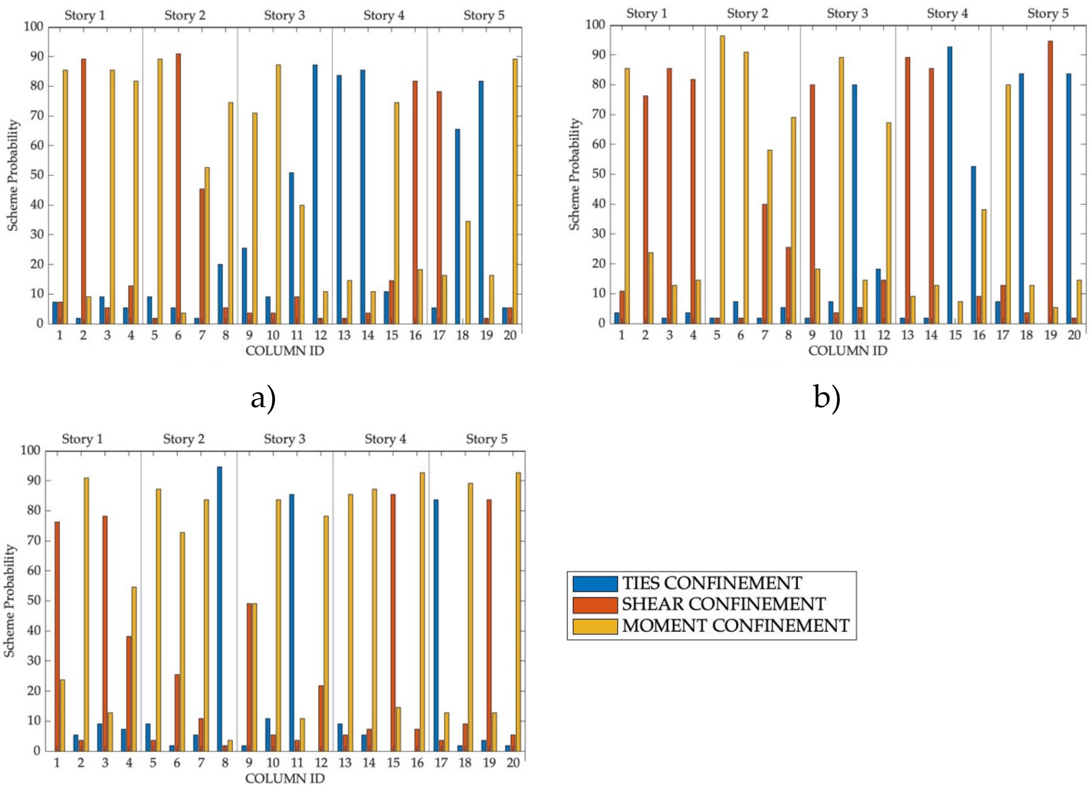

a) b)

c)

Figure 31 Probability of confinement of column for case study A: a) no elite member b) one elite member c) two elite members

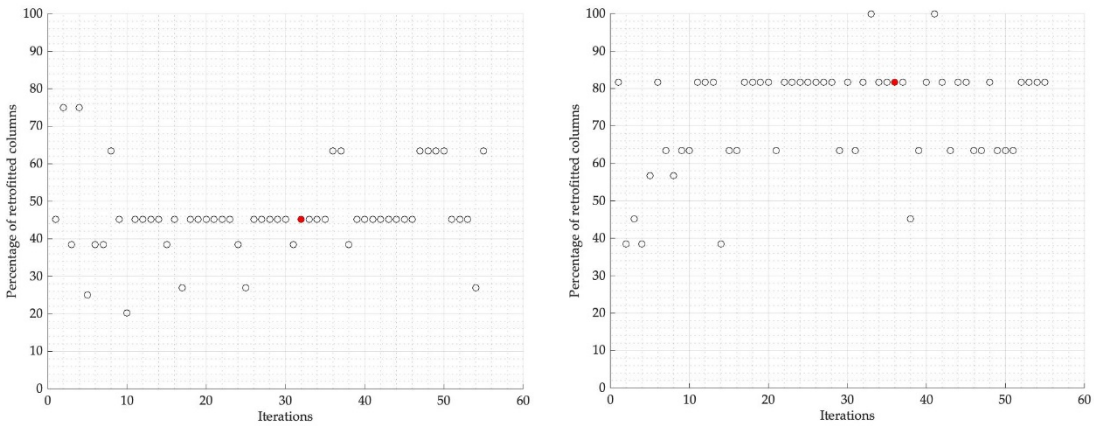

a) b)

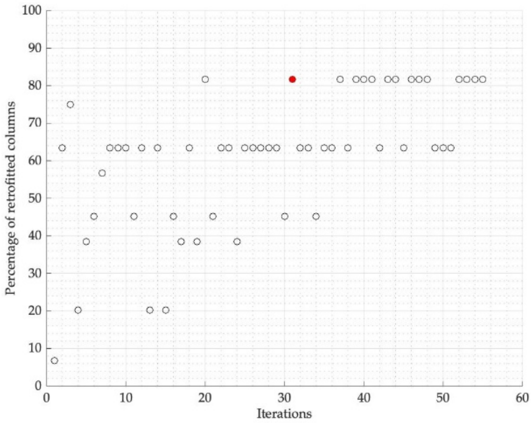

c)

Figure 32 Percentage of material used for the first story case study A: a) no elite member b) one elite member c) two elite members

4.3.2 Results of case study B

Subjecting each of the frames to NTHA within the loop of the genetic algorithm, the configuration of the optimal FRP layout is found and they are depicted in the following figures, where an optimal configuration of FRP strategy is found for each single ground motion input.

4.3.2.1 Case B1

The archetype model of a 4 RC space frame structure exhibit an improvement in the seismic performance as the expected reduction of the inter-story drift is found after each run of the genetic algorithm, which are depicted in Figure 33 and Figure 34, for both components. Analyzing the output, a uniform distribution of the horizontal displacement is noticeable which is expected as it has been defined by the penalty function expressed in Equation (31).

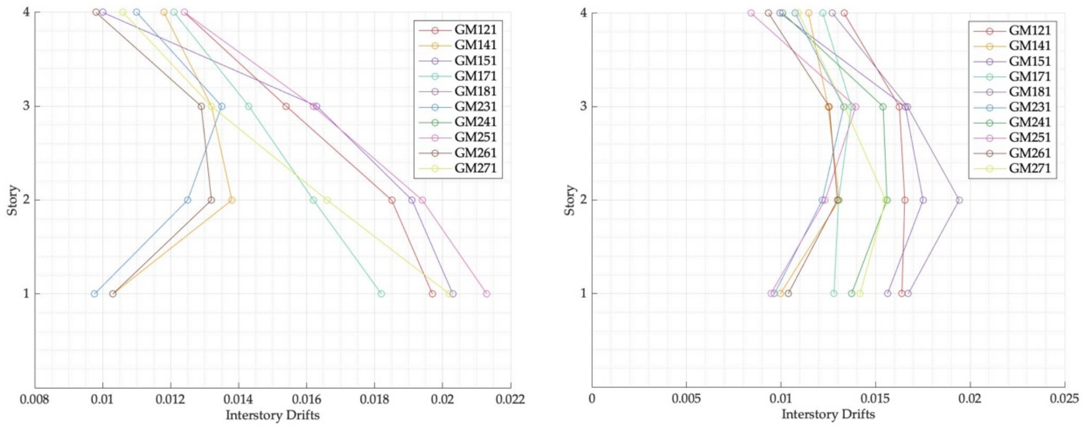

a) b)

Figure 33 Inter-Story drifts by component 1 of case B1: a) Bare structure b) Optimal Retrofitted structure

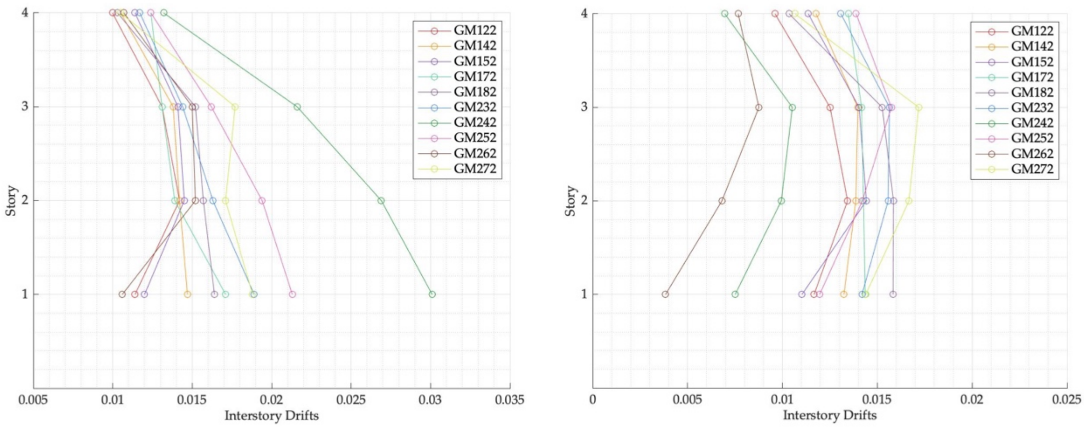

a) b)

Figure 34 Inter-Story drifts by component 2 of case B1: a) Bare structure b) Optimal Retrofitted structure

The retrofitting of joints is herein analyzed by the changes along each iteration of the generic algorithm. In this particular case, Figure 35 and Figure 36 depicts the percentage of confinement of inner and outer joints for GM181 and GM271, respectively. As outer joints are confined to a lesser degree in comparison with inner joints, as this latter are found to confined by an extra beam, it is expected that an optimal scheme regarding the joints strengthening will lead to the placement of FRP on outer joints, meaning a higher probability of FRP usage in this location. However, as one of the particular problems within evolutionary algorithm is that a solution is determined by the convergence of the problem; therefore, it is contemplated that is some cases the expected result is not achieve, as is depicted in Figure 35b. By extracting each optimal layout regarding joints strengthening, Figure 36 shows the results for each seismic event where a trend of confinement outer joints is depicted in a greater extend for both ground motion input, far-fault and near-fault.

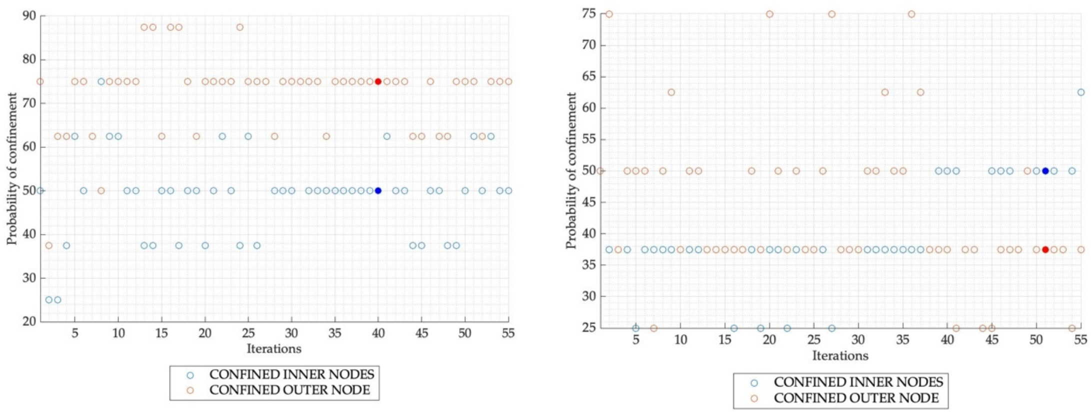

a) b)

Figure 35 Retrofitting of joints of case B1: a) Confinement record by GM181 b) Confinement record by GM271

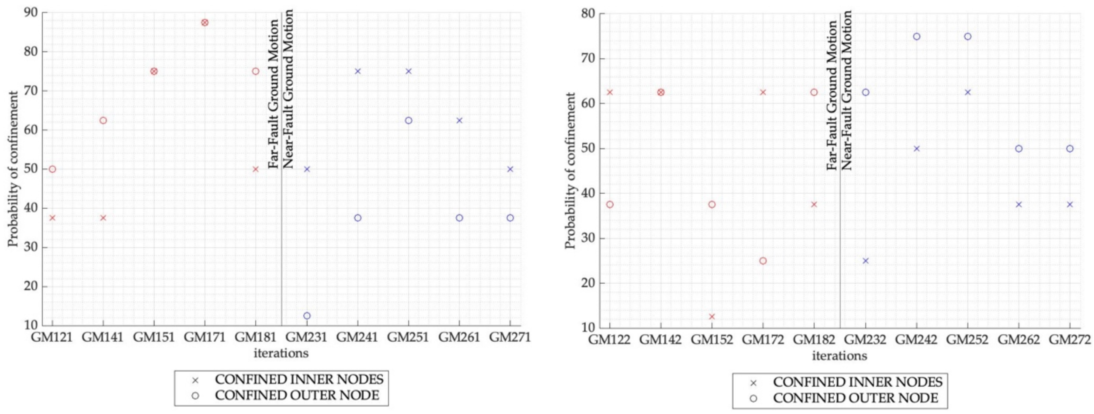

a) b)

Figure 36 Retrofitting of joints of case B1: a) trend by component 1 b) trend by component 2

4.3.2.2 Case B2

For the 12 story frame structure, the optimal configuration for each case depicts an improvement in the interstory drift for each quake, but in some cases a non uniform distribution is still not found, Figure 37 and Figure 38, but still a reduction of the coefficient of variation is obtained, see Table 12. The issue regarding the extend of uniform interstory drift can be addressed to the increment of the solution domain in the genetic algorithm in comparison to the previous evaluation of case B1. Nontheless, the enhacement of seismic performance is still noticeable after implementing the FRP retrofitting technique, where the reduction of the maximum inter-story drift is around 70% in some ground motion inputs, see Table 11.

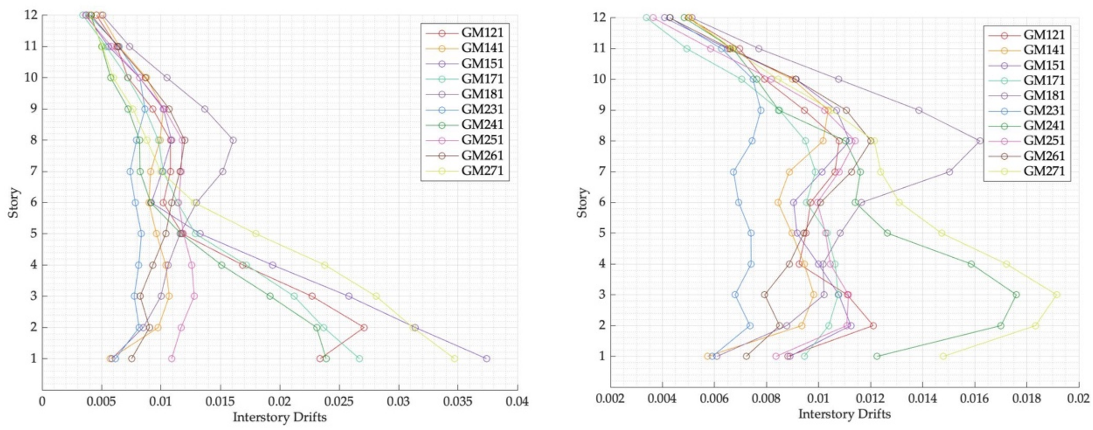

a) b)

Figure 37 Inter-Story drifts by component 1of case B2 : a) Bare structure b) Optimal Retrofitted structure

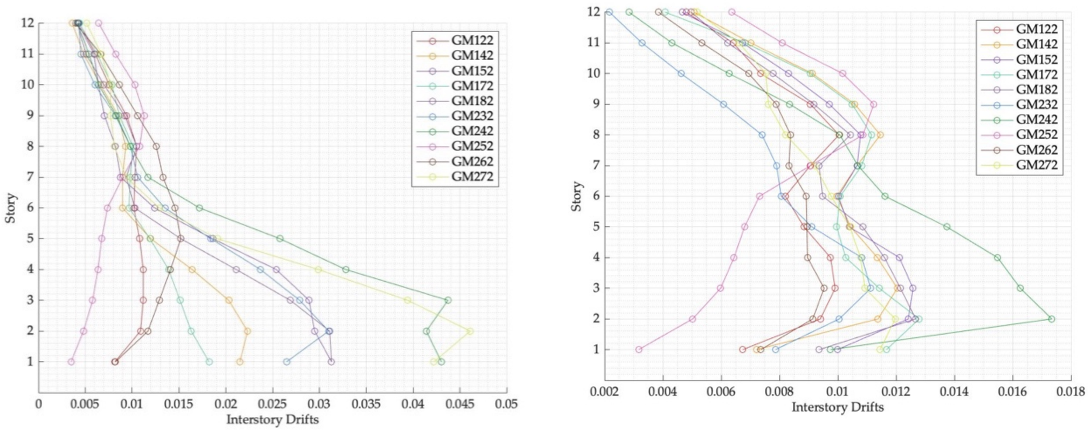

a) b)

Figure 38 Inter-Story drifts by component 2 of case B2: a) Bare structure b) Optimal Retrofitted structure

Figure 39 depicts the same ground motions iteration history regarding the joints strengthening as case B1; however, in this case the expected results is found where the outer joints have a higher probability to be retrofitted. Nonetheless, in a general perspective, Figure 40 shows the trend for each seismic event where the joints a retrofitted in the same extend depending on the quake input.

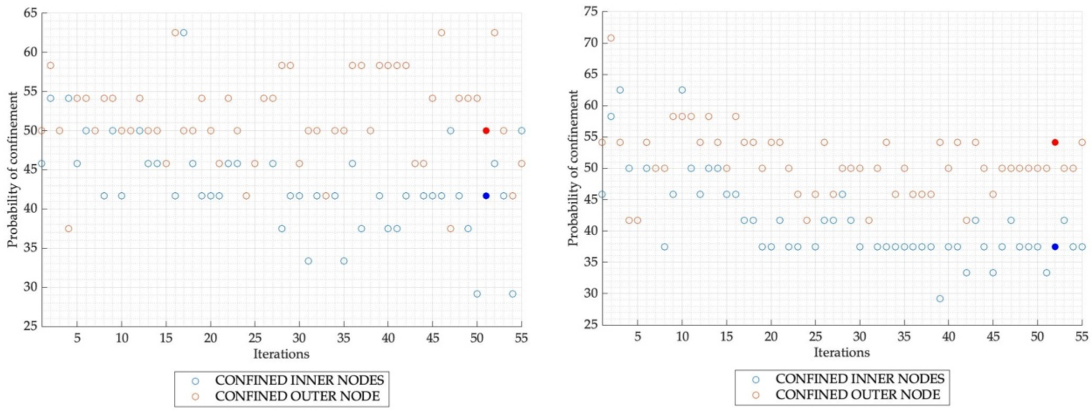

a) b)

Figure 39 Retrofitting of joints of case B2: a) Confinement record by GM181 b) Confinement record by GM271

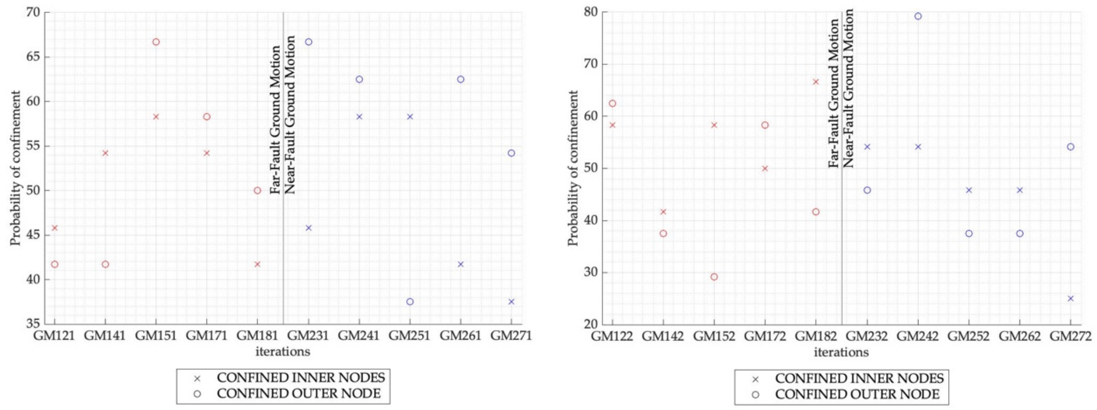

a) b)

Figure 40 Retrofitting of joints of case B2: a) trend by component 1 b) trend by component 2

4.3.2.3 Case B3

The latest results regards to case B3, the modified archetype model in order to present height irregularities. As case B2, the reduction of the maximum inter-story drift is achieved and in a certain degree, the coefficient of variation drops with respect to the original structure, see Table 11 and Table 12. A reduction of the horizontal displacement reach a value around 70% for some input event with the optimal configuration of the FRP sheets.

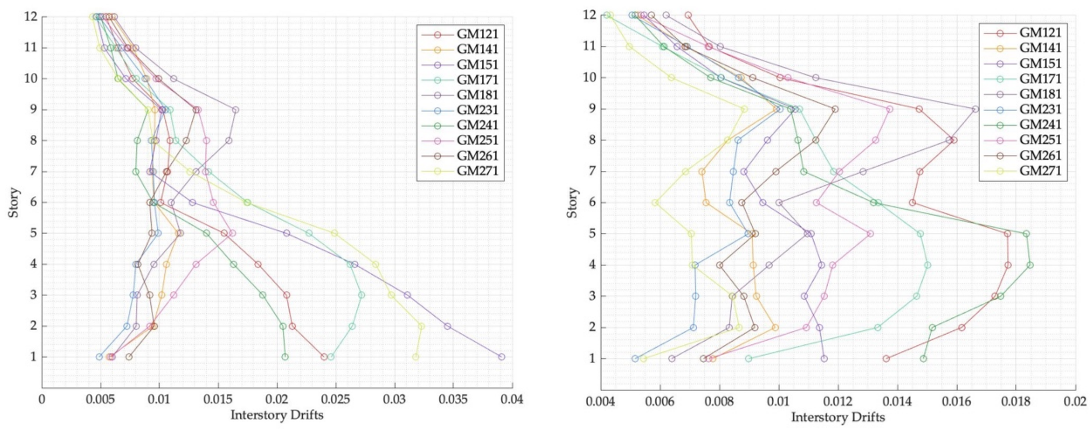

a) b)

Figure 41 Inter-Story drifts by component 1 of case B3: a) Bare structure b) Optimal Retrofitted structure

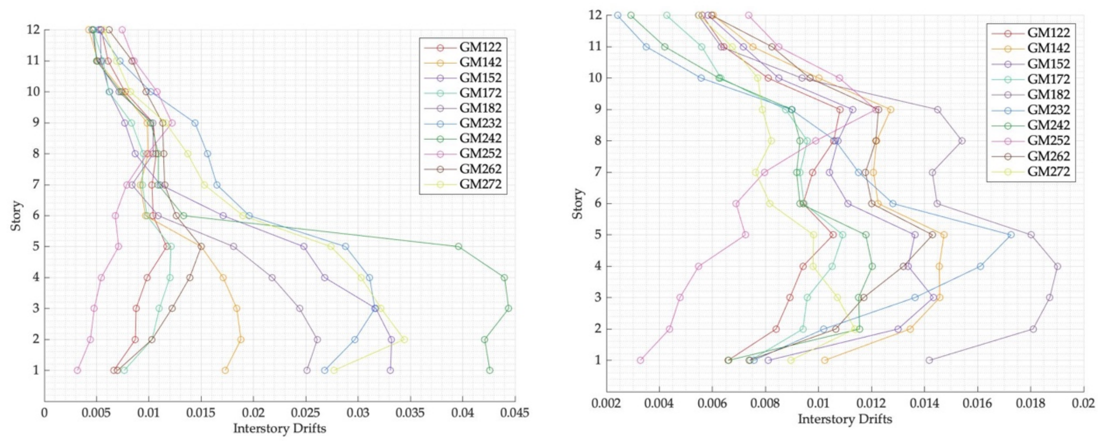

a) b)

Figure 42 Inter-Story drifts by component 2 of case B3: a) Bare structure b) Optimal Retrofitted structure

For the modified frame model, the expected results regarding GM181 and GM271 are found following the expected trend of greater probability of outer confinemened joints within the the iteration record, Figure 43. By analyzing the results of each ground motion in case B3 regarding joints strengthening, the global trend is to retrofit the outer joints, Figure 44.

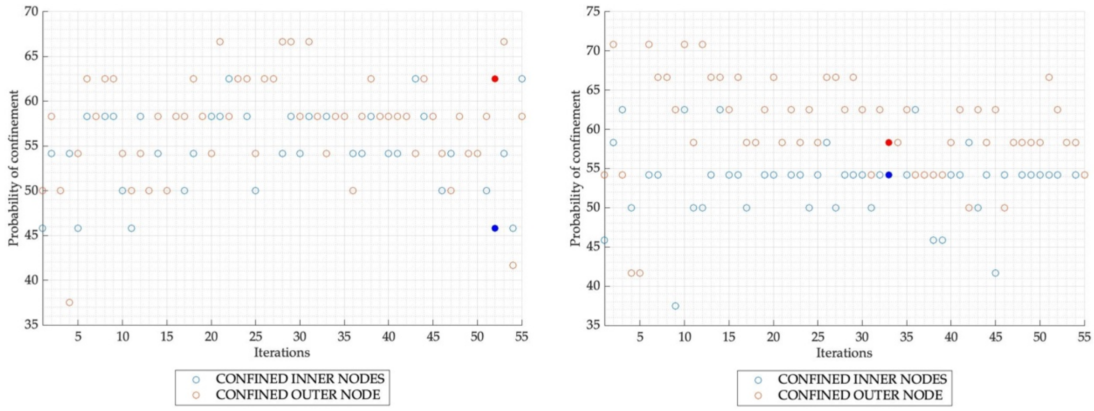

a) b)

Figure 43 Retrofitting of joints of case B3: a) Confinement record by GM181 b) Confinement record by GM271

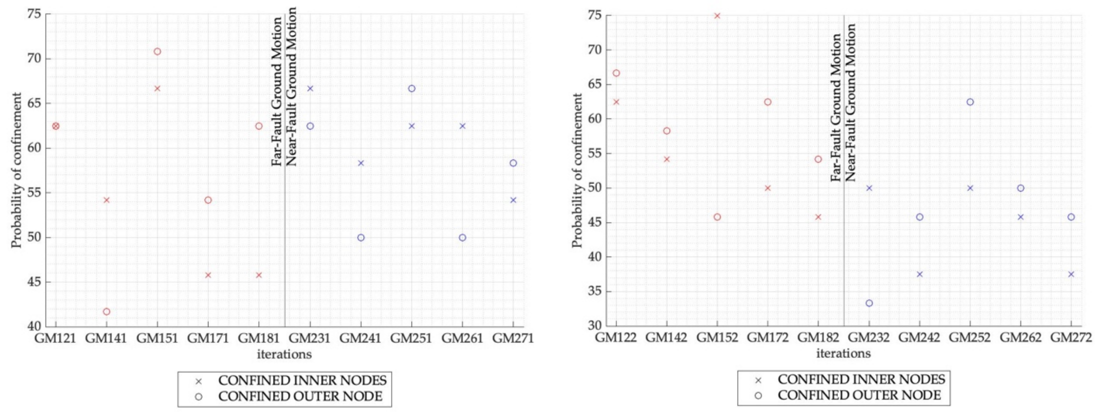

a) b)

Figure 44 Retrofitting of joints of case B3: a) trend by component 1 b) trend by component 2

Finally, as this latter frame introduces height irregularities regarding the variation of the story's clearance, Figure 45 depicts the proneness of FRP material to be located in a specific structural column and with a given wrapped scheme. It is shown that the material is located around the stories 5, 9 and 12 where the height have been modified. Therefore, it is noticeable that the proneness of the strategy's output is to retrofit this latter stories.

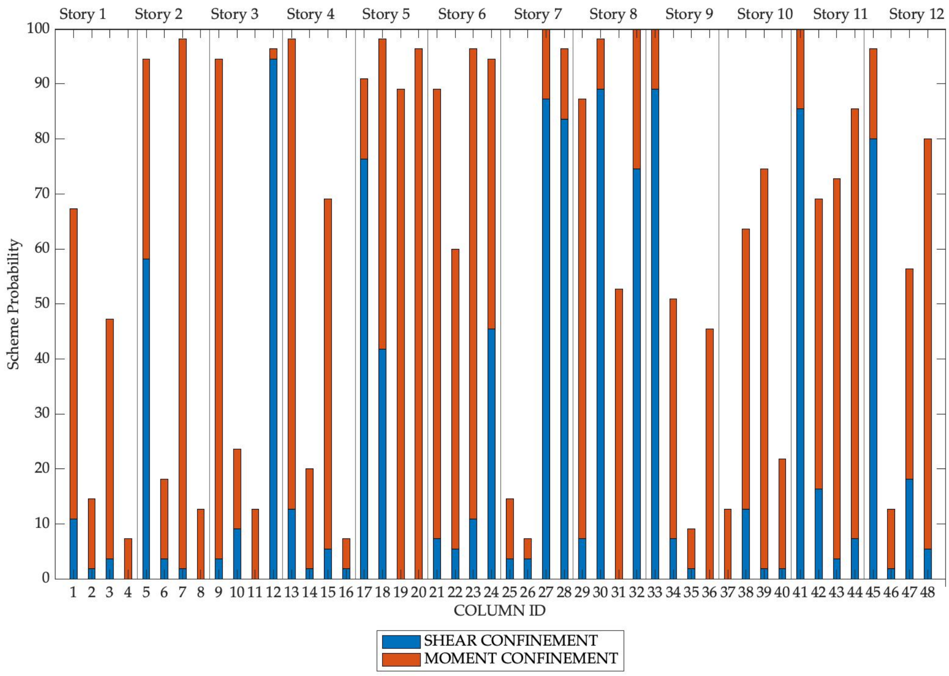

Figure 45 Proneness of FRP material in columns of frame B3 of Far Fault GM181

Table 11 Percentage of inter-story drift reduction

Model	Component	GM12	GM14	GM15	GM17	GM18	GM23	GM24	GM25	GM26	GM27
B1	1	16.80	5.29	23.00	29.67	21.46	1.33	35.54	55.59	1.67	29.80
	2	5.42	9.93	0.55	16.02	3.48	24.92	75.05	43.85	55.20	23.46
B2	1	55.35	8.22	76.23	64.61	0.00	10.16	48.74	12.89	0.00	57.35
	2	11.52	48.97	68.08	35.88	70.10	67.58	62.79	0.62	41.18	74.03
B3	1	43.25	21.55	70.51	46.14	0.00	4.29	28.16	19.20	9.16	73.16
	2	9.83	28.46	60.84	9.75	30.69	56.87	74.08	0.33	4.67	66.95

Table 12 Ratio of coefficient of variation

Model	Component	GM12	GM14	GM15	GM17	GM18	GM23	GM24	GM25	GM26	GM27
B1	1	0.49	0.91	0.81	0.28	0.75	0.99	0.83	1.03	1.02	0.52
	2	0.90	0.54	1.18	0.20	0.96	0.42	0.63	0.49	1.56	0.86
B2	1	0.38	0.94	0.32	0.48	0.97	0.80	0.60	0.92	0.98	0.51
	2	0.83	0.41	0.35	0.63	0.37	0.62	0.58	1.01	0.69	0.29
B3	1	0.58	0.86	0.30	0.63	0.97	0.85	0.76	0.73	0.88	0.35
	2	0.88	0.54	0.39	0.89	0.58	0.96	0.46	0.99	0.94	0.36

4.3.3 Comparison of uniform and optimal layout of FRP

A common strategy is to retrofit the first stories of a regular building with no differences in heights, comparing the seismic performance of an uniform layout and the optimal layout allows us to determine the benefits from the approach. Herein, case B2 is selected to be uniformly retrofitted in the first two stories and to check the difference between the results of the optimal retrofiting strategy given by the above mentioned approach.

By setting the same parameters of FRP sheets and performing the NTHA of each ground motion, we obtained the results depicted in Figure 46 and Figure 47 for Far Fault and Near Fault ground motions, respectively. The juxtaposition of these latter results brings a better understanding of how the optimal strategy is benefitial concerning an uniform configuration of FRP in terms of inter-story drift. Although Near Fault input ground motion shows an improvement to a lesser extent than Far Fault seismic events, both results show in a general overview an improvement of the seismic performance.

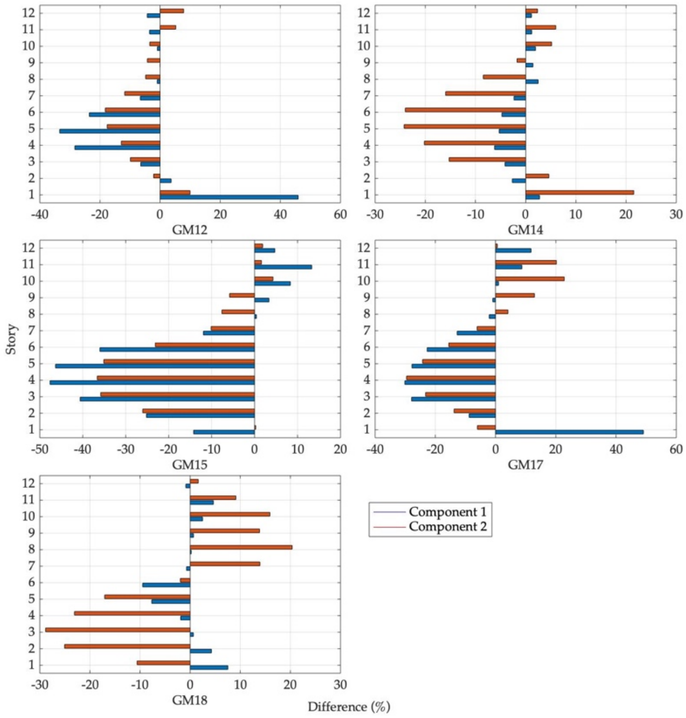

Figure 46 Inter-story drift comparison of uniform and optimal configuration of FRP layout due to Far Fault ground motions

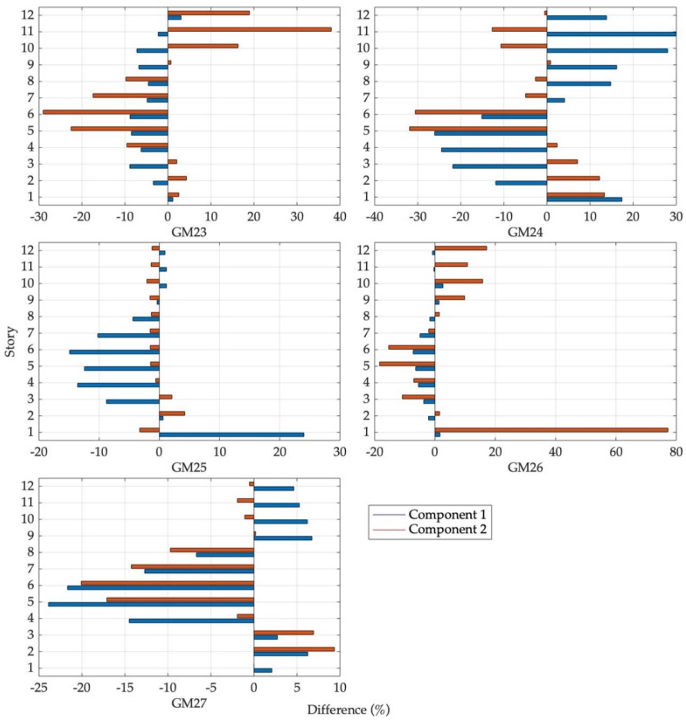

Figure 47 Inter-story drift comparison of uniform and optimal configuration of FRP layout due to Near Fault ground motions

4.4 Application of retrofitting in columns and joints

One of the important aspect of retrofitting is the feasibility of strategy. Fiber-reinforced polymer excel in this matter due to its lightweight and manuverability in situ. Herein, a brief overwiew of the physical implementation of FRP retrofitting stretagy is described for both, columns and joints. The following views are representative to case study B. The following FRP configurations are recommendation by guidelines (FEMA (Federal Emergency Management Agency) 2006). Nonetheless, the lack of documented strengthening techniques addressed the following layout schemes to those used in literature (Ilki et al. 2013).

4.4.1 Fiber-reinforced polymer application in columns

The placement of FRP sheets around the rectangular RC columns is straightforward as some low invasive treatment must be taken into account as removal of part of infills. This allows to increase the ease of implementation of the jacketing.

A set of CFRP wraps with a thickness and width of 0.34 mm and 100 mm is used to retrofit the column by considering a nil overlapping of sheets as it covers the entire column's length for the case of shear confinement, and a define length for moment confinement, which is evaluated by Equation (27). Figure 48 depicts an external column with a set of sheets following the previous description.

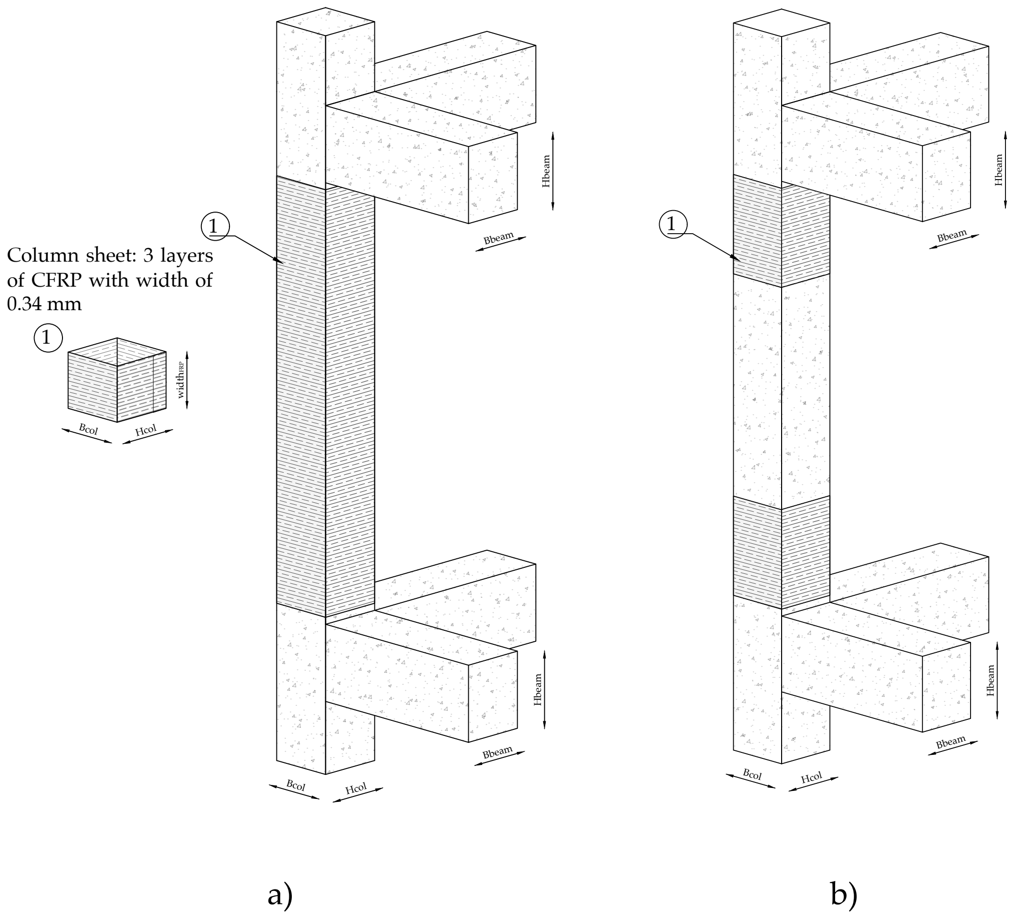

Figure 48 Columns retrofitting application: a) shear confinement b) moment confinemet

4.4.2 Fiber-reinforced polymer application in joints

For joints strengthening, a set of sheets with a width of 0.50 mm are chosen to retrofit the panel zone which are declare as non-conforming, this is done by placing the sheets beyond the panel zone as shown in Figure 49 for the case of corne joints which are considered the lesser confined. The wrap sheet at the end of the elements allow to avoid the delamination of the CFRP sheet which are indentified by the tag ID 3 and 4 (Parvin and Granata 2000).

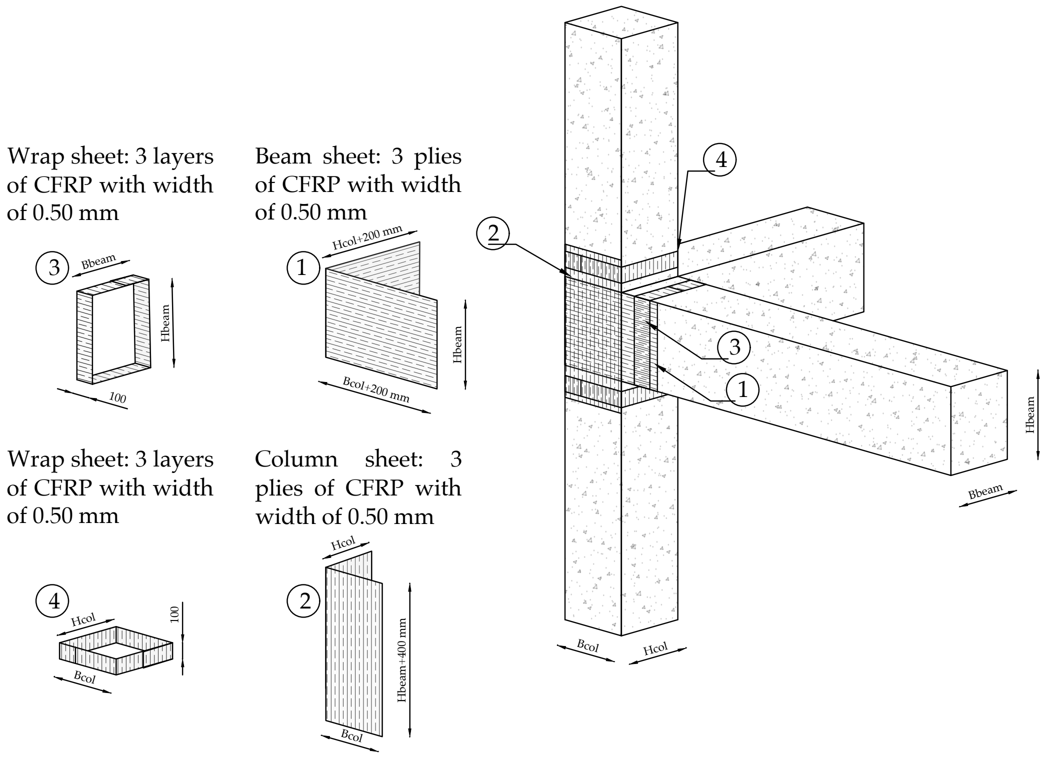

Figure 49 Joints retrofitting application of corner joint

The exterior inner joint is strengthen by setting a shown in Figure 50, where the panel zone sheet is wrapped with the layout given by the tag ID 2, which can be either b wrapping the beams of the columns ends. Noticing that this requires the invasive methodoly of removing either non-structural elements or part of the slab.

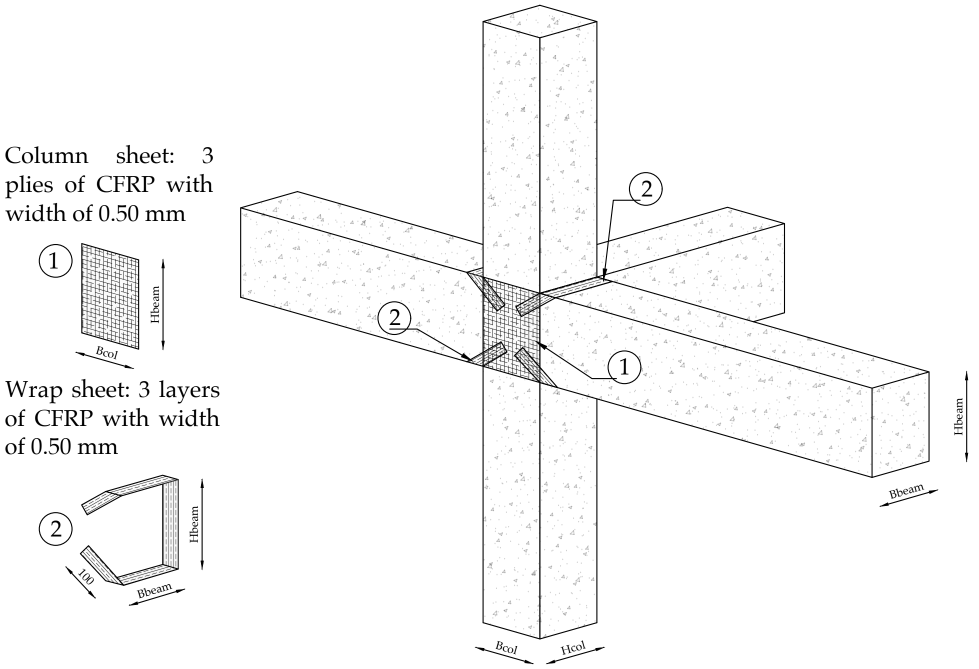

Figure 50 Joints retrofitting application of exterior joint - three beam connection

Conclusion and future work

The approach permits locating the FRP material in an optimal configuration to reduce the inter-story drift. Considering this aspect and comparing short and long period buildings, the retrofitted joints' location has been proven to be more accurate in the expected place (corner joints) when assessed in tall buildings.

The methodology proves better results with Far Fault ground motions input. Nonetheless, further evaluation and refinement of the models could obtain better results with Near Fault seismic events.

In terms of inter-story drifts, the obtained reduced horizontal displacements reach values up to 70%, which indicates a significant improvement in seismic performance.

Concerning the uniform distribution of inter-story intention, the structures exhibit an improvement in the uniformity on average; nonetheless, this latter presents a more significant enhancement in long-period buildings, clearly depicted by some of the four-story ratios buildings that were higher than the unity.

Lastly, the uniform retrofitting strategy and the optimal configuration of the twelve-story building structure were juxtaposed. Despite the lesser improvement extent in Near Fault ground motion's horizontal displacement, both NTHA yield enhancement in the mentioned structure. Hence, the application of the optimal strategy brings a new approach to retrofit structures avoiding to resort to time consuming assessment regarding the different possible FRP configurations.

Nonetheless, new aspects can be develop forward to improve the algorithm features as improving the model structure by increasing the level of detail can enhance the convergence to an optimal value to avoid the local deficiencies (e.g. bar slips in joints, mass irregularity, plan irregularity). Moreover, adding the shear effect in columns to link it with a shear curve to exploit the shear confinement.

Moreover, infills are also known to develop a different seismic performance that should be model meticulously; therefore, the influence of infills, although neglected in this particular case, should be studied in future work.

In terms of the optimization approach, implemented genetic algorithm can be juxtaposed with other evolutionary algorithms in this particular retrofitting strategy to contrast the speediness of these metaheuristic approaches (e.g. the use of Particle Swarm).

Appendix A

A comparison between fibers and polymeric matrix mechanical properties is found in Table 13. In Table 14, a juxtaposition of FRP properties and fibers is described.

Table 13 Fiber and matrix mechanical properties

Material	Elastic Modulus (GPa)	Tensile Strength (MPa)	Ultimate Tensile Strain (%)
Carbon			
High strength	215 - 235	3500 - 4800	1.4 - 2.0
Ultra high strength	215 - 235	3500 - 6000	1.5 - 2.3
High modulus	350 - 500	2500 - 3100	0.5 - 0.9
Ultra high modulus	500 - 700	2100 - 2400	0.2 - 0.4
Glass			
E	70	1900 - 3000	3.0 - 4.5
S	85 - 90	3500 - 4800	4.5 - 5.5
Aramid			
Low modulus	70 - 80	3500 - 4100	4.3 - 5.0
High modulus	116 - 130	3500 - 4000	2.5 - 3.5
Polymeric matrix	2.7 - 3.6	40 - 82	1.4 - 5.2

Table 14 Comparison between fiber and FRP mechanical properties (Monti and Petrone 2018)

Pre-cured systems	Modulus of elasticity		Ultimate strength		Ultimate strain	
	[GPa]		[MPa]		[%]	
	FRP	Fibre	FRP	Fibre	FRP	Fibre
	E_{FRP}	E_{fib}	F_{FRP}	f_{fib}	ε_{fu}	$\varepsilon_{fib,u}$
CFRP (low modulus)	160	210 - 300	2800	3500 - 4800	1.6	1.4 - 2.0
CFRP (hig modulus)	300	350 - 500	1500	2500 - 3100	0.5	0.4 - 0.9

Bibliography

Standards

ACI (American Concrete Institute) (2007). "Report on fiber-reinforced polymer (FRP) reinforcement for concrete structures." *ACI 440R-07*, Farmington Hills, MI: ACI.

ACI (American Concrete Institution) (2017). "Guide for the design and construction of externally bonded FRP systems for strengthening concrete structures." *ACI Committee 440.2 R-17*, Farmington Hills, MI: ACI.

ASCE (American Society of Civil Engineers) (2017). "Minimum design loads and associated criteria for buildings and other structures." *ASCE/SEI 7-16*, American Society of Civil Engineers.

CNR (Council National Research) (2013). "Instructions for the Design, Execution and Control of Static Consolidation Interventions using FRP (in Italian - Istruzioni per la Progettazione, l'Esecuzione ed il Controllo di Interventi di Consolidamento Statico mediante l'utilizzo di Compositi Fibrorinforzati)." *DT200/2013*.

EN (European Committee for Standardization) (2005). "Eurocode 2: Design of structures for earthquake resistance-part 1: general rules, seismic actions and rules for buildings." Brussels: European Committee for Standardization.

EN (European Committee for Standardization) (2005). "Eurocode 8: Design of structures for earthquake resistance-part 1: general rules, seismic actions and rules for buildings."

EN (European Committee for Standardization) (2005). "Eurocode 8: Design of structures for earthquake resistance-Part 3: Assessment and retrofitting of buildings." Brussels: European Committee for Standardization.

FEMA (Federal Emergency Management Agency) (2006). "Techniques for the seismic rehabilitation of existing buildings." *Building Seismic Safety Council for the Federal Emergency Management Agency*, FEMA 547.

fib (2001). "Externally bonded FRP reinforcement for RC structures." *Technical Report, Task Group 9.3—FRP Reinforcement for Concrete Structures*, International Federation for Structural Concrete.

fib (2006). "Retrofitting of concrete structures by externally bonded FRPs, with emphasis on seismic applications." International Federation for Structural Concrete.

fib (2007). "FRP reinforcement in RC structures." International Federation for Structural Concrete.

Ministero Delle Infrastrutture e dei Trasporti (2018). "Norme Tecniche per le Costruzioni." Gazzetta Ufficiale Serie Generale.

Articles

Beydokhti, E. Z., and Shariatmadar, H. (2016). "Strengthening and rehabilitation of exterior RC beam–column joints using carbon-FRP jacketing." *Materials and Structures*, 49(12), 5067-5083.

Chisari, C., and Bedon, C. (2016). "Multi-Objective Optimization of FRP Jackets for Improving the Seismic Response of Reinforced Concrete Frames." *American Journal of Engineering and Applied Sciences*, 9(3), 669-679.

Chisari, C., and Bedon, C. (2017). "Performance-based design of FRP retrofitting of existing RC frames by means of multi-objective optimisation." *"Bollettino di Geofisica Teorica ed Applicata"*, 58.

Choi, S. W. (2017). "Investigation on the seismic retrofit positions of FRP jackets for RC frames using multi-objective optimization." *Composites Part B: Engineering*, 123, 34-44.

Choi, S. W., Kim, Y., and Park, H. S. (2014). "Multi-objective seismic retrofit method for using FRP jackets in shear-critical reinforced concrete frames." *Composites Part B: Engineering*, 56, 207-216.

Cosgun, C., Cömert, M., Demir, C., and İlki, A. (2019). "Seismic Retrofit of Joints of a Full-Scale 3D Reinforced Concrete Frame with FRP Composites." *Journal of Composites for Construction*, 23(2).

De Risi, M. T., Ricci, P., Verderame, G. M., and Manfredi, G. (2014). "A Nonlinear Macro Model For Numerical Simulation Of Exterior Rc Joints Without Transverse Reinforcement."

Farinazzo, A. (2019). "Building Resilience and Sustainability Concrete Structures with the use of FRP."Master Thesis, Politecnico di Torino.

Hassan, W. M., and Moehle, J. P. "A cyclic nonlinear macro model for numerical simulation of beam-column joints in existing concrete buildings." 24-28.

Hassanat, A., Almohammadi, K., Alkafaween, E., Abunawas, E., Hammouri, A., and Prasath, V. B. (2019). "Choosing mutation and crossover ratios for genetic algorithms—a review with a new dynamic approach." *Information*, 10(12), 390.

Ilki, A., Demir, C., and Comert, M. (2013). "Retrofit of RC joints with FRP composites." *Proc., APFIS*.

Ilki, A., and Kumbasar, N. (2003). "Compressive behaviour of carbon fibre composite jacketed concrete with circular and non-circular cross-sections." *Journal of Earthquake Engineering*, 7(03), 381-406.

Kucukkoc, I., Karaoglan, A. D., and Yaman, R. (2013). "Using response surface design to determine the optimal parameters of genetic algorithm and a case study." *International Journal of Production Research*, 51(17), 5039-5054.

Lam, L., and Teng, J. (2002). "Strength models for fiber-reinforced plastic-confined concrete." *Journal of structural engineering*, 128(5), 612-623.

Lam, L., and Teng, J. G. (2003a). "Design-oriented stress–strain model for FRP-confined concrete." *Construction and Building Materials*, 17(6-7), 471-489.

Lam, L., and Teng, J. G. (2003b). "Design-oriented stress-strain model for FRP-confined concrete in rectangular columns." *Journal of reinforced plastics and composites*, 22(13), 1149-1186.

Liel, A. B. (2008). *Assessing the collapse risk of California's existing reinforced concrete frame structures: metrics for seismic safety decisions*.

Mahdavi, G., Nasrollahzadeh, K., and Hariri-Ardebili, M. A. (2019). "Optimal FRP Jacket Placement in RC Frame Structures Towards a Resilient Seismic Design." *Sustainability*, 11(24).

Mazzoni, S., McKenna, F., Scott, M. H., and Fenves, G. L. (2006). "OpenSees command language manual."

Mitra, N., and Lowes, L. N. (2007). "Evaluation, calibration, and verification of a reinforced concrete beam–column joint model." *Journal of Structural Engineering*, 133(1), 105-120.

Parvin, A., and Granata, P. (2000). "Investigation on the effects of fiber composites at concrete joints." *Composites Part B: Engineering*, 31(6-7), 499-509.

Pohoryles, D. A., Melo, J., Rossetto, T., Varum, H., and Bisby, L. (2019). "Seismic retrofit schemes with FRP for deficient RC beam-column joints: State-of-the-art review." *Journal of Composites for Construction*, 23(4), 03119001.

Scott, M. H. (2011). "Numerical integration options for the force-based beam-column element in OpenSees." *Force-Based Element Integration Options in OpenSees*, 1-7.

Spoelstra, M. R., and Monti, G. (1999). "FRP-confined concrete model." *Journal of composites for construction*, 3(3), 143-150.

Teng, J. G., Jiang, T., Lam, L., and Luo, Y. Z. (2009). "Refinement of a design-oriented stress–strain model for FRP-confined concrete." *Journal of Composites for Construction*, 13(4), 269-278.

Tsonos, A. G., and Stylianidis, K. (2002). "Seismic Retrofit of Beam-to-Column Joints with High-Strenght Fiber Jackets." *European Earthquake Engineering*, 16(2), 56-72.

Zou, X. K., Teng, J. G., De Lorenzis, L., and Xia, S. H. (2007). "Optimal performance-based design of FRP jackets for seismic retrofit of reinforced concrete frames." *Composites Part B: Engineering*, 38(5-6), 584-597.

Books

Adeli, H., and Sarma, K. C. (2006). *Cost optimization of structures: fuzzy logic, genetic algorithms, and parallel computing*, John Wiley & Sons.

Chakrabarti, A., Menon, D., and Sengupta, A. K. (2008). *Handbook on seismic retrofit of buildings*, Alpha Science International, Limited.

Kramer, O. (2017). *Genetic algorithm essentials*, Springer.

Monti, G., and Petrone, F. (2018). "Strengthening of RC Buildings with Composites." *Strengthening and Retrofitting of Existing Structures*, Springer, Singapore, 163-180.

Priestley, M. J. N., Seible, F., and Calvi, G. M. (1996). *Seismic design and retrofit of bridges*, John Wiley & Sons.

Electronic references

Istituto Nazionale di Geofisica e Vulcanologia (INGV) (2007). "Progetto DPC." <http://esse1-gis.mi.ingv.it>. (28/11, 2020).

PEER (Pacific Earthquake Engineering Research Center) (2014). "NGA-West2 Research Project." *Earthquake Spectra*, <https://ngawest2.berkeley.edu>. (3, 30).

Softwares

Cimellaro, G. P., and Marasco, S. (2015). "A computer-based environment for processing and selection of seismic ground motion records: OPENSIGNAL." *Frontiers in Built Environment*, 1, 17.

MATLAB. version 9.7.0.1471314 (R2019a). The MathWorks Inc.

Open system for earthquake engineering simulation (OPENSEES). 2000. version 3.2.2.

SeismoMatch. version V21. SEISMOSOFT Earthquake Engineering Software Solutions.

SeismoSelect. version V21. SEISMOSOFT Earthquake Engineering Software Solutions.

SeismoStruct. version V21. SEISMOSOFT Earthquake Engineering Software Solutions.